Reduction of Capacity Drop at Sag and Tunnel Bottlenecks through Connected Vehicles

Master thesis

by

Ying Wu

to obtain the degree of Master of Science in Civil Engineering
at Delft University of Technology,
to be defended publicly on August 15^{th}, 2023 at 15:00h

Student number:	5491363	
Project duration:	December 6, 2022 – August 15, 2023	
Thesis committee:	Prof. dr. ir. Bart van Arem,	CiTG, TU Delft, Chair
	Dr. ir. Irene Martínez Josemaría,	CiTG, TU Delft, Daily supervisor
	Dr.ir. Andreas Hegyi,	CiTG, TU Delft, External supervisor

An electronic version of this thesis is available at `http://repository.tudelft.nl/`.

TU Delft Delft University of Technology

Preface

Dear reader,

This thesis is the culmination of my intense two-year academic journey: obtaining a Master of Science degree in Transportation and Planning from Delft University of Technology. This work represents a fusion of acquired knowledge and developed skills during my master's study. I am delighted to have had the opportunity to delve into a subject that resonates with my interest - using connected vehicles to address the capacity drop problem.

I am deeply grateful for the guidance and support of my esteemed committee members, Prof. Bart van Arem and Dr.ir. Andreas Hegyi, whose expertise has been invaluable in shaping the direction of this research. Additionally, my daily supervisor, Dr. ir. Irene Martínez Josemaría has provided unwavering encouragement and insights that have been essential to this work's development.

I wish to wholeheartedly thank my parents and brother for being my unwavering support throughout these two years of studying in a foreign land. To my dear friends, your care and concern have provided a steady source of comfort and the cherished memories of our shared joyful moments will forever be etched in my heart.

Furthermore, I extend my appreciation for the capabilities of CHATGPT, which have contributed to improving the language.

As I present the culmination of my efforts, I hope that this exploration contributes to the ongoing discourse on traffic management, connected vehicles, and the quest for more efficient and sustainable urban mobility. This journey of inquiry and discovery underscores the dynamic nature of scientific exploration and the limitless possibilities that lie ahead.

Ying Wu
Delft, August 2023

Abstract

Traffic congestion is a challenge that frequently emerges due to changes in the roadways such as tunnels and sags, causing capacity reduction. The capacity drop phenomenon exacerbates traffic congestion, due to decreased queue discharge rates. Among the strategies employed for traffic management, Variable Speed Limit (VSL) control is a common approach to alleviate congestion and mitigate capacity drop. The control is expected to be more powerful when integrated with Connected Vehicles (CVs). However, the intricate interplay between the Market Penetration Rate (MPR) of CVs and the parameters governing VSL remains under-explored.

This study seeks to quantify the relationship between the MPR of CVs and the key VSL parameters, encompassing factors like the optimal acceleration length and speed limits. The VSL control is applied to CVs at the road section upstream of a tunnel bottleneck modelled by a continuum car-following model with bounded acceleration. The findings of this research suggest a minimum MPR of CVs essential for preventing capacity drop and reaching the maximal outflow. Intriguingly, this challenges the conventional notion that regulating solely the leading vehicle suffices to govern the behaviour of all following vehicles. The value of the minimum MPR threshold is affected by the acceleration behaviours exhibited by vehicles.

Furthermore, this study underscores the importance of considering the MPR of CVs when devising the optimal speed limit and acceleration length for the VSL. It shows that while a higher speed limit can lead to higher throughput, the optimal acceleration length increases exponentially with the increasing speed limit, particularly in cases with low MPR of CVs. While adopting a relatively lower speed limit, the acceleration length can be reduced to 0m for all levels of MPR of CVs. In summary, it suggests that when implementing VSL in practice, a balance between the resulted throughput, the required acceleration length and the robustness of VSL across different levels of MPR of CVs should be considered.

Nomenclature

Abbreviations

Abbreviation	Definition
VSL	Variable speed limit
CVs	Connected vehicles
NCVs	Non-connected vehicles
MPR	Market penetration rate
ATM	Active traffic management
V2I	Vehicle-to infrastructure
I2V	Infrastructure-to-vehicle
V2V	Vehicle-to-vehicle
CBA	Constant bounded acceleration
LWR	Lighthill-Whitham-Richards

Symbols

Symbol	Definition	Unit
L	Bottleneck length	[m]
$\tau(x)$	Time gap at location x	[seconds]
$q(x,t)$	Flow rate at location x at time t	[veh/h]
$k(x,t)$	Density at location x at time t	[veh/km]
v_f	Free flow speed	[km/h]
k_j	Jam density	[veh/km]
C_1	Normal road capacity	[veh/h]
C_2	Bottleneck capacity (before congestion)	[veh/h]
C_3	Dropped capacity (after congestion)	[veh/h]
$A_{max}(x,v)$	Bounded acceleration rate at location x with the speed of v	[km/h^2]
$a(x,v)$	The real-time acceleration rate at location x with the speed of v	[km/h^2]
a_0	Maximum acceleration rate on a level road	[km/h^2]
g	Gravitational acceleration	[m/s^2]
$\Phi(x)$	The decimal grade at x	/
$V(x,k)$	The speed-density fundamental diagram	[km/h]
n_v	The number of simulated real vehicles	/
t_f	The simulation time	[s]
Δ_t	Simulation time step	[s]
Δ_n	Discretization of real vehicles	/
D_1	Constant low demand	[veh/h]
D_2	Constant high demand	[veh/h]
$s(t,n)$	Spacing between n^{th} vehicle and $(n-1)^{th}$ vehicle	[m]
s_j	Jam spacing	[m]
VSL	Speed limit of VSL	[km/h]
k_{VSL}	Density imposed by a speed limit in VSL zone	[veh/km]
C_{VSL}	The controlled flow by VSL	[veh/h]

Symbol	Definition	Unit
VSL_{max}	The maximal speed limit	[km/h]
VSL_{min}	The minimal speed limit	[km/h]
v_2	Speed located on a congested branch of the downstream fundamental diagram and corresponds to a controlled traffic flow C_{VSL}	[km/h]
$-L_a$	The end location of the VSL zone	[m]
$\|L_a\|$	The acceleration length from the end of the VSL zone to the entrance of the bottleneck	[m]
$T(n)$	The time when the n^{th} real vehicle passes the end of bottleneck	[s]

Contents

1 Introduction

Traffic congestion is a significant issue, often caused by low-capacity bottlenecks like sags and tunnels. The capacity drop phenomenon worsens traffic conditions with the reduced queue discharge rate. One of the traffic management strategies is Variable speed limit (VSL) control, which holds promise for congestion relief and capacity drop prevention, particularly with connected vehicles (CVs). However, the impact of the market penetration rate (MPR) of CVs on VSL parameters is not fully understood. This research aims to quantify the relationships between the MPR of CVs and VSL parameters, such as speed limit and optimal acceleration length. By adjusting VSL parameters, based on different MPR levels of CVs, the study aims to prevent capacity drop and enhance traffic conditions.

1.1. Background

Traffic congestion is a common problem plaguing the world, and frequently occurs on highways, expressways, and major roadways during peak travel times. It negatively impacts commuting speeds, increases total travel time, and contributes to higher levels of particulate pollutants (Robinson, 1984). Traffic congestion is a complex phenomenon influenced by multiple interrelated factors. It arises from various causes, including but not limited to a high volume of vehicles, traffic signals, traffic accidents, road construction and bottlenecks. Bottlenecks specifically refer to constrained areas like narrow roads, bridges, tunnels, or other infrastructure where traffic flow becomes restricted. These areas often experience congestion as vehicles slow down or wait for their turn to pass through. Notably, sags and tunnels are critical bottlenecks, especially in mountainous regions (Koshi et al., 1992). Sags consist of sections where the road slopes downwards, followed by an uphill section, while tunnels are subterranean passages. A study by Xing et al. (2014) revealed that intercity expressways in Japan experience nearly 80% of traffic congestion, with 60% occurring at sags or uphills and 20% happening at tunnel entrances. Road capacity is the maximum potential traffic volume that a roadway can accommodate, considering the prevailing road conditions. Sag and tunnel bottlenecks generally have a lower capacity than normal road sections. Research conducted by Koshi (1985) and Koshi et al. (1992) demonstrates that the capacity of a normal road segment is typically around 2000-2250 vehicles per hour per lane (vphpl). However, when encountering a sag or tunnel bottleneck, the roadway's capacity decreases even without congestion, typically reaching around 1500 vphpl. Consequently, fewer vehicles can traverse the bottleneck compared to a regular road section.

A noteworthy traffic phenomenon that exacerbates traffic congestion is the capacity drop that occurs at bottlenecks (Hall and Agyemang-Duah, 1991; Koshi et al., 1992; Chen and Ahn, 2018). The capacity drop denotes a situation where the discharge rate of the congestion is lower than the maximum traffic flow, i.e., the road capacity (Yuan et al., 2017). It occurs when queues form upstream of the bottleneck. As vehicles approach the bottleneck and subsequently accelerate out of the queues, their driving behaviour is affected by congestion, resulting in reduced traffic flow. This leads to the underutilization of roadway capacity and worsening traffic congestion. According to the studies conducted by Koshi (1985) and Koshi et al. (1992), after queues form at bottlenecks, the capacity of the roadway experiences a further drop due to the capacity drop phenomenon. The resulting capacity typically ranges between 1200 and 1400 vphpl and is influenced by factors such as the location, length, and gradient

of the bottlenecks.
Despite being recognized for many years (Koshi et al., 1992), capacity drop at sags and tunnels remains a persistent problem. To tackle this problem, researchers have proposed various control strategies aimed at preventing or mitigating the capacity drop (Goñi-Ros et al., 2014; Xing et al., 2007; Sun et al., 2018). Among these strategies, one of the most promising approaches for reducing congestion and enhancing traffic flow at these bottlenecks is the implementation of the VSL control (Hegyi et al., 2005; Papageorgiou et al., 2008; Hegyi and Hoogendoorn, 2010; Sadat and Celikoglu, 2017). VSL is an active traffic management (ATM) strategy that utilizes dynamically adjustable speed limit signs to regulate traffic flow in response to high demand or congested conditions. It proactively controls the inflow into bottlenecks, preventing queues from forming within them. By dynamically adjusting the speed limit to create gaps between vehicles, VSL helps to alleviate existing congestion.
VSL system consists of detectors, controllers, and actuators, working in conjunction to regulate traffic flow. Traffic monitoring devices are employed in VSL as detectors (e.g. sensors and cameras), to collect real-time traffic data. The collected data is transferred to the controller, where it is processed to estimate current traffic states. Based on predetermined rules and thresholds (e.g., in open-loop VSL) or advanced control laws (e.g., in rule-based VSL), the controller generates control signals. These signals consider factors such as traffic volume, congestion levels, road conditions, and specific objectives set. Control signals are then sent to actuators and are usually converted into speed limit instructions for drivers in traditional VSL. The actuator can be integrated into various traffic control devices located upstream of bottlenecks such as electronic signs, variable message signs, or overhead gantries. When the demand is below the bottleneck capacity and congestion is resolved, the VSL system raises the speed limit back to the default speed limit (i.e., free-flow speed) (Khondaker and Kattan, 2015). The field of VSL control has seen significant research efforts to maximise its effectiveness in improving traffic conditions. Scholars have analyzed various factors that influence the control performance of VSL. These factors include the control laws used to determine control signals (Van den Hoogen and Smulders, 1994; Chen et al., 2014), the VSL application location (Martínez and Jin, 2020), driver compliance with control signals (Hellinga and Mandelzys, 2011), traffic heterogeneity (Li et al., 2022), measurement errors in traffic data collection (Alasiri et al., 2021), and transmission delays of information among VSL components.
CVs, namely automobiles equipped with wireless communication capabilities, are expected to be a game-changing technology that has revolutionized the way we think about VSL traffic control management (Lu et al., 2014; Khondaker and Kattan, 2015; Han et al., 2017; Wang et al., 2016; Letter and Elefteriadou, 2017). CVs can serve as both actuators and detectors, offering a cost-effective alternative to traditional road facilities like gantries and loop detectors. Through wireless communication systems, CVs enable efficient and accurate transmission of traffic conditions and control information between vehicles and control systems (Khondaker and Kattan, 2015). Specifically, by utilizing embedded sensors, CVs can capture the trajectories of individual vehicles and the surrounding environment, allowing for precise data collection. This information can be transmitted to the VSL controller through Vehicle-to-Infrastructure (V2I) communication, enabling real-time adjustments to control signals. Furthermore, CVs can receive updated traffic information and personalized driving instructions via Infrastructure-to-Vehicle (I2V) communication. These include dynamic speed limits, real-time traffic conditions, and potential hazards. By providing drivers with advanced information, CVs empower them to make informed driving decisions in advance, enhancing safety and overall driving efficiency. However, the effectiveness of these technologies depends on the MPR of CVs (Lee and Park, 2013; Han et al., 2017), which denotes the percentage of CVs among all vehicles on the road. Simulation experiments conducted by Lee and Park (2013) demonstrated that a higher MPR leads to greater reductions in travel time.
While existing studies have confirmed the impact of MPR of CVs on the overall performance of control systems, the specific influence of MPR of CVs on the VSL parameters, such as the speed limit and the control application location, remains unexplored. Strategies for adjusting the parameters of the VSL system in a CV environment to ensure control effectiveness are lacking. Therefore, it is crucial to investigate and bridge these gaps to maximize the benefits of implementing CV technology in VSL control strategies.
This chapter provides a background of the research topic and outlines the problem the study aims to address. To guide the research process, a research objective and a set of research questions have been formulated based on the identified problem. Furthermore, the scope of the study and its overall structure are presented at the end of this chapter.

1.2. Research objectives and research questions

The integration of CVs into VSL control presents a promising opportunity to enhance traffic throughput by effectively preventing capacity drop in bottleneck areas. Through timely wireless communication and the utilization of CVs as detectors and actuators, more synchronized and streamlined traffic management can be achieved (Lee and Park, 2013; Grumert and Tapani, 2020). To fully harness the potential of CVs in VSL systems, it is essential to explore strategies for integrating CVs and study their interaction dynamics with VSL strategies. The MPR of CVs has been identified as a significant factor affecting traffic dynamics and overall VSL control performance (Lee and Park, 2013; Han et al., 2017). Therefore, it is crucial to further analyze and quantify the impact of MPR of CVs on VSL systems and develop compensatory strategies for any adverse effects, ensuring that VSL systems can operate effectively even with varying levels of CV penetration.
This thesis aims to identify and quantify the interrelationships between specific parameters of the VSL control system and the MPR of CVs. By understanding this relationship, we can determine the minimum MPR of CVs required for efficient traffic management in different scenarios. Additionally, our goal is to fine-tune the parameters of the control system based on varying MPR levels to ensure its effectiveness in preventing capacity drop and optimizing throughput at bottlenecks. By achieving these objectives, the study provides valuable insights into harnessing the benefits of CV technology for enhancing traffic conditions and contributing to effective traffic management practices.
Based on research gaps and research objectives, the main research question can be stated as follows:

Main research question:

How does the MPR of CVs affect the determination of parameter values for CVs-based VSL to ensure effectiveness in preventing capacity drop at sag and tunnel bottlenecks?

To answer the main question, four sub-questions are developed. The sub-questions will be addressed orderly. And, we will be able to answer the main question to reach the research objective.
Sub questions:

- What is the current state-of-the-art of using CVs in VSL to prevent capacity drop? Are there any limitations or challenges that need to be addressed before this technology can be fully implemented?
- Which existing models are best suited to modelling vehicle behaviour and capacity drop in sag and tunnel bottlenecks for this study? What assumptions and simplifications of the models are necessary?
- What are key parameters in the VSL design that need to be considered when implementing a CV-based open-loop VSL control strategy, and how do these parameters interact?
- What is the minimum MPR of CVs to enable an open-loop VSL to achieve the maximal flow in the study's context? What variables impact this minimum MPR value?
- How can the VSL parameters be adjusted considering different MPR of CVs to prevent capacity drop at sag and tunnel bottlenecks?
- What is the impact of assumptions made in modelling and simulations on research results?

1.3. Research scope

The research involves the use of VSL to prevent the capacity drop phenomenon at sag and tunnel bottlenecks. The main objective is to find the optimal values of parameters of VSL to enhance bottleneck throughput in different MPR of CVs environments. The study focuses on two parameters interacting with the MPR of CVs: the speed limit in the VSL zone and the acceleration length for vehicles from the end of the VSL zone to the entrance of the bottleneck. It is important to note that the VSL control exclusively applies to CVs in this study, assuming full compliance from all CVs, while non-connected vehicles (NCVs) operate in a car-following mode. This work also helps to analyse the influence of driver compliance on VSL control indirectly. In this context, the MPR of CVs can be regarded as the driver compliance rate.
The study takes a microscopic perspective, exploring the impact of the changing geometry of the single-lane road and the longitudinal behaviour of the former vehicles on the behaviour adaptation of the

following vehicles. The research seeks to understand how these factors contribute to the capacity drop phenomena at the bottleneck. However, lateral movements such as lane changes and overtaking behaviours are not considered.
Traffic control levels can be categorized into four hierarchies: network, link, platoon, and vehicle levels. The network level manages the entire system, the link level handles specific locations, the platoon level coordinates groups of vehicles, and the vehicle level controls individual vehicles (Wang, 2014). Both link-level and vehicle-level controls are included in this study, as individual vehicle behaviour (i.e., speed and positions) and overall traffic dynamics (i.e., flow and density) in the bottleneck road section are analyzed. Control signals are transmitted between link-level and vehicle-level controllers (i.e., CVs) via V2I/I2V communication. This direct communication allows for the delivery of control information without relying on road-based actuators, as indicated by the dashed line in Fig 1.1. Additionally, the study does not include communication between vehicles through Vehicle-to-Vehicle (V2V) communication.

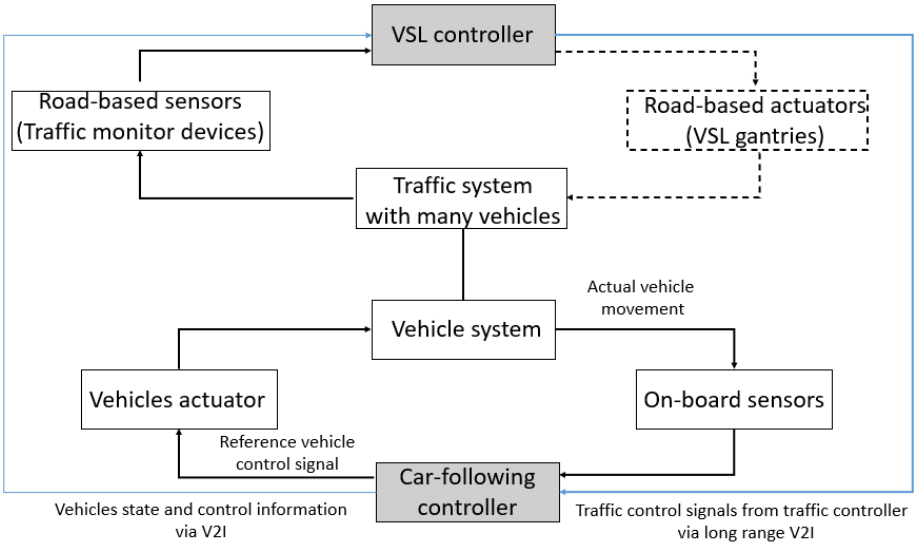

Figure 1.1: Schematic representation of the control problem (Wang et al., 2016)

The study does not develop a specific control algorithm for VSL to adjust the control signals based on real-time traffic conditions. Instead, a static open-loop VSL control is implemented in the tunnel bottleneck simulation, considering an exogenous demand pattern that remains constant over time. The VSL parameters are simulation inputs, which are predetermined for different scenarios to realize a controlled simulation environment.
The traffic flow at the end of bottlenecks serves as a performance indicator for assessing traffic conditions and evaluating the effectiveness of control strategies. Additionally, the study includes the measurement and comparison of travel times for individual vehicles and average travel times through the specific road section in different scenarios. This analysis aims to demonstrate the improvements in traffic efficiency achieved by implementing the VSL control strategy.

1.4. Research outline

Chapter 2 presents a review of relevant literature. It explores traffic dynamics at sag and tunnel bottlenecks, examining the factors that contribute to capacity drop phenomena. Then, it reviews and compares existing traffic models built to replicate this phenomenon, aiming to find the most suitable model for this research. The literature review also covers the various VSL control strategies employed, both with and without CVs. The inspiration for this research from the literature is summarised at the end. Chapter 3 focuses on describing the methodologies utilized in the study. It describes mathematical formulations of the adopted traffic flow model and explains how it reproduces the behaviour of vehicles at sag and tunnel bottlenecks. Additionally, it details the simulation methods to apply VSL control in the CVs environment, highlighting the methods to investigate VSL parameters and specifying assumptions made during the research. Chapter 4 provides an overview of calibrated values for the models obtained from the literature and describes the simulation initialization. Furthermore, it outlines

the design of the analyzed scenarios, each serving a specific purpose within the research framework. Chapter 4 includes a convergence analysis, which validates the accuracy and reliability of the simulation results. The chapter then proceeds to present the simulation results for each scenario. It analyzes and interprets simulation results, providing insights into the relationship between the MPR of CVs and the parameters of the VSL control. Chapter 5 serves as a sensitivity analysis, examining the impact of bottleneck length, bounded acceleration assumptions, and transmission delay of VSL on the VSL control performance. It also evaluates how the random order of CVs within the platoon affects the capacity drop occurrence when the MPR of CVs is fixed. The final chapter serves as a conclusion and reflection of the research. It summarizes the key findings and provides conclusive answers to the research questions. The chapter reflects on the research process, discussing limitations encountered and suggesting potential areas for improvement. The conclusion also offers recommendations for future research directions.

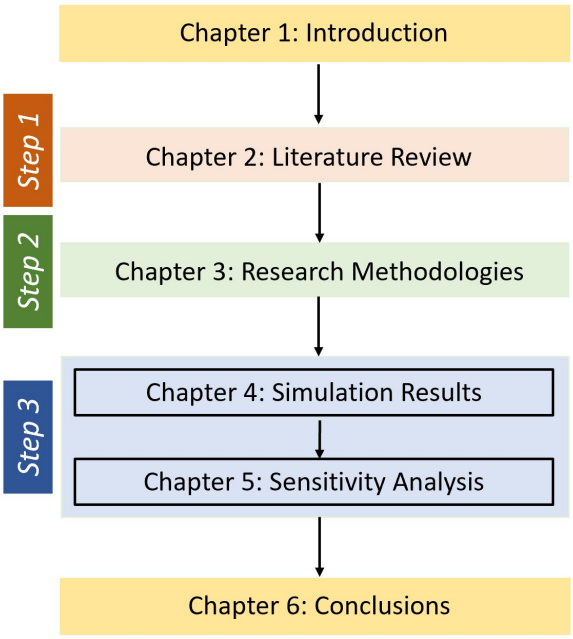

Figure 1.2: Research outline

2

Literature review

In this chapter, we conduct a review of the relevant literature. Section 2.1 focuses on the unique traffic dynamics observed in sag/tunnel bottlenecks compared to regular road sections. It provides some explanation for these dynamics from microscopic and macroscopic perspectives. Moving forward, section 2.2 lists various traffic models proposed in the literature to capture these specific traffic dynamics and reproduce capacity drop phenomena observed in sag/tunnel bottlenecks. These models are reviewed in terms of their assumptions, methodologies, advantages, and limitations, with the ultimate goal of identifying the most appropriate traffic model for this research. Next, section 2.3 starts with analyzing traditional VSL systems that utilize gantries. The objective is to gain insights into determining key parameters of VSL and identifying their relationships. Building on this, the section also delves into the literature exploring the methodologies for integrating CVs into VSL systems. It further encompasses research evaluating the performance of CVs-based VSL control systems in preventing capacity drop. Additionally, specific attention is given to investigating the influence of the MPR of CVs on the overall control performance.

2.1. Traffic dynamics and capacity drop in sag and tunnel bottlenecks

Sags and tunnels are critical bottlenecks in roads, affecting traffic dynamics and causing congestion. The literature provides valuable insights into the reasons and mechanisms behind these low capacities and congestion phenomena. Early in the 1990s, Koshi et al. (1992) conducted an analysis based on traffic data collected in Japanese motorway tunnels and upstream sections of sags. They observed that tunnels and sags lead to traffic congestion even at lower volumes compared to regular road sections. The capacity further decreases as queues form and grow. They identified a transition period from free flow to congested flow, typically taking less than 10 minutes after drivers enter a queue. Lighting conditions were found to influence departure flow rates, with higher rates observed in brighter conditions. This work was expanded upon in a subsequent study by Koshi (2003). They argued that drivers maintain their car-following spacing even when the speed reduces due to changing environments, resulting in a reduced flow rate. They quantified this reduction, which depends on the time spent in the queue, light conditions (day or night), and other factors. Brilon and Bressler (2004) collected traffic data from freeway upgrades in Germany and conducted microscopic simulations to analyze traffic dynamics. Their findings indicated that road capacity is not constrained by the length of the gradient but depends solely on the degree of the gradient. Travel velocity, on the other hand, is notably affected by the degree of the gradient, the length of the upgrade, and the presence of trucks. Using a driving simulator on intercity expressways, an analysis was conducted by Yoshizawa et al. (2012) to assess how road alignments, namely sags and tunnels, and the driving behaviour of the leading vehicle, influence the behaviour of following vehicles. They found that road alignments had a more pronounced influence on driver behaviour of following drivers compared to the behaviour of the leading vehicle.

Goñi-Ros et al. (2013) investigated congestion in sags with a special focus on the fast and slow lanes. They observed that congestion typically originates in the fast lane(s) of the uphill section and spreads to the slow lane(s) during high traffic demand. The research utilized traffic data collected from a sag in

Japan. By analyzing vehicle trajectories and examining the relationship between average time headway and speed on the fast lanes at different locations, the study revealed that both car-following inhomogeneous characteristics (i.e., longer headways on the uphill section compared to the downhill section at similar speeds) and the frequency of lane changes contribute to congestion formation. However, comparing the frequency of these two causes indicated that car-following inhomogeneous characteristics were the primary factor, while disruptive lane changes had a lesser impact. Jin (2017) found that the bounded acceleration capability of vehicles at sag/tunnel bottlenecks results in capacity drop. They introduced vehicles' bounded acceleration on the LWR (Lighthill-Whitham-Richards) stationary states inside the lane-drop zone of the lane-drop bottlenecks as an additional constraint for the optimization formulation of the entropy condition and demonstrated that the optimization problem is uniquely solved with well-defined instantaneous continuous standing waves, comprised of the LWR stationary states inside the lane-drop and the bounded acceleration stationary states in the downstream acceleration zones. Further research conducted by Jin (2018) revealed that capacity drops can still occur in single-lane bottlenecks, indicating that lane changes are neither a necessary nor sufficient condition for the capacity drop. To avoid the need to model lane-changing effects, this study focuses on studying capacity drop at single-lane sag and tunnel bottlenecks.

Table 2.1: Reviewed literature about traffic dynamics in sag/tunnel bottlenecks

Paper	Methodology	Conclusion
Koshi et al. (1992)& Koshi (2003)	Traffic data analysis in motorway tunnels	Observing lower queue discharge rate than road capacity; Congested caused by increased gradients or changes in light conditions
Brilon and Bressler (2004)	Microscopic simulations	Road capacity is determined by the degree of the gradient, not the length of the gradient
Yoshizawa et al. (2012)	Driver simulators	Road alignments have a stronger impact on following vehicle behaviours compared to the leading vehicle behaviour
Goñi-Ros et al. (2013)	Traffic data analysis in a sag	Congestion begins at fast lanes and spreads to slow lanes; Congestion is caused by longer headway on uphill sections more frequently than lane-changing behaviour
Jin (2017) & Jin (2018)	The traffic model design and calibration	Capacity drop caused by the bounded acceleration of vehicles; Capacity drop occurs in the single lane

2.2. Traffic flow models to reproduce capacity drop in sag and tunnel bottlenecks

Researchers have developed a range of traffic flow models to reproduce the capacity drop phenomena observed in bottleneck areas. These models vary from microscopic models that focus on individual vehicle behaviour to macroscopic models that analyze aggregate variables, catering to different research objectives (Marczak et al., 2015; Haut et al., 2005; Wada et al., 2020). As discussed in section 2.1, the capacity drop observed in sag and tunnel bottlenecks is a multifaceted phenomenon influenced by intricate interactions among the geometry characteristics, the traffic conditions, and the behaviour adaptation of individual vehicles (Koshi, 2003; Brilon and Bressler, 2004; Yoshizawa et al., 2012; Goñi-Ros et al., 2013; Jin, 2018). By employing different assumptions, these models prioritize capturing the diverse factors that can influence individual driver behaviour and lead to the capacity drop.

One of the earliest car-following models was developed by Helly (1959). It models the traffic in the single-lane tunnel bottleneck. The model consists of a reaction time-lagged system of differential equations. They assumed a linear relationship between the acceleration rate and the relative speed and headway distance. Koshi et al. (1992) proposed hypothetical mathematical models of car-following in free flow and congested flow, respectively. They assumed different levels of driver tension in congested and free-flow states and assumed that drivers would not adjust their acceleration to compensate for environmental factors in congested flows. However, this assumption is not supported by empirical evidence in car-following driving experiments. Based on traffic data from uphill gradients in German freeways, Treiber et al. (2000) observed the traffic states which were localized or extended, homogeneous or oscillating. Combined states were observed as well, like the coexistence of moving localized clusters and clusters pinned at road inhomogeneities, or regions of oscillating congested traffic upstream of nearly homogeneous congested traffic. They conducted simulations using the "intelligent driving model", which is a continuous microscopic single-lane model using empirical data as boundary conditions. Using one parameter to capture the inhomogeneities of local variations, this model can

reproduce all observed phenomena, including the coexistence of states, qualitatively. Goñi-Ros et al. (2016) introduced a microscopic traffic model which incorporates a car-following model considering the impact of freeway gradient on vehicle acceleration. The model assumes that drivers compensate for any increase in freeway gradient linearly over time with a maximum gradient compensation rate defined by a model parameter. The validity of the model is assessed through a simulation study conducted at a sag on a Japanese freeway. The simulation results, compared to previous empirical data, show that the model accurately reproduces important traffic phenomena at sags. These phenomena include a reduced capacity compared to normal sections, the bottleneck location near the end of the vertical curve, and the capacity drop caused by congestion. Jin (2018) presents a behavioural kinematic wave model (KW model) that explains the bottleneck effects in sags and tunnels. A location-dependent triangular fundamental diagram is proposed to explain the capacity reduction effect from the assumption of an increased linear time gap to capture a larger spacing at the same speed. The capacity drop occurs due to a bounded acceleration rate constraint. It also captures the associated low acceleration rate when vehicles accelerate away from the upstream queue. The resulting low acceleration rate out of the upstream queue is verified by the structure of continuous standing waves in speed. The model is calibrated and validated using four stationary vehicle trajectories at the Kobotoke tunnel in Japan, and the theoretical predictions closely match the observed data. Thus, despite its inability to describe rather complicated phenomena such as the probabilistic capacity reduction and stop-and-go traffic upstream of bottlenecks (Goñi Ros et al., 2014) at the current stage, this simplified model can be a suitable building block for a more comprehensive theory. However, the KW model has a limitation in its assumption that ”capacity drop stationary states” are immediately reached upon the onset of congestion. In reality, there exists a transition period to reach this stationary traffic state, characterized by persistent congestion where flow, speed, and acceleration processes are nearly stationary and stable (Koshi et al., 1992; Ozaki, 2003). KW model fails to explain the formation and stabilization of the stationary state. To compensate for this limitation, Wada et al. (2020) proposed a continuum car-following model with the same assumptions as the KW model, i.e., location-dependent time gaps and bounded acceleration. They use a one-dimensional iterated function system to model the formation of the capacity drop and capture its dynamic characteristics. This model is derived from an analysis of the spatial pattern of equilibrium and bounded acceleration traffic states observed in a lead-vehicle problem. By utilizing this model, they uncover a range of properties associated with the capacity drop, including its existence, uniqueness, global convergence, and transition time.

Table 2.2: Reviewed literature about traffic flow models to reproduce capacity drop

Paper	Assumptions	Model
Helly (1959)	A linear relationship between the acceleration rate and the relative speed and headway distance	A car-following model consists of a reaction time-lagged system of differential equations
Koshi et al. (1992)	Different levels of driver tension in congested and free-flow states; No adjustment on acceleration when congested	Hypothetical mathematical car following models
Treiber et al. (2000)	/	A continuous microscopic single-lane intelligent driving model with empirical boundary conditions
Goñi-Ros et al. (2016)	Drivers compensate for the increase in freeway gradient linearly with a maximum gradient compensation rate defined by a model parameter	A microscopic car-following model considering the impact of freeway gradient on vehicle acceleration
Jin (2018)	A location-dependent triangular fundamental diagram; Bounded acceleration	A behavioural kinematic wave model
Wada et al. (2020)	A location-dependent triangular fundamental diagram; Bounded acceleration	A continuum car-following model

In this thesis, the model of Wada et al. (2020) is adopted to simulate the capacity drop phenomenon in a single-lane traffic scenario within a tunnel bottleneck. Though this model fails to reproduce the stop-and-go wave and the probabilistic capacity reduction, it effectively reproduces the capacity drop phenomenon and accurately represents its essential characteristics, like the transition period of the capacity drop and an accurate value of the dropped capacity after carefully calibrating the parameters of the bounded acceleration model. Notably, the model requires only a few parameters for calibration and validation, and these parameters hold clear physical interpretations. This simplicity of the model

facilitates the explanation of the underlying mechanisms that lead to the capacity drop. The geometry data from the Kobotonoke Tunnel bottleneck in Japan is utilized for calibrating and validating the model (Koshi et al., 1992).

2.3. Traffic management based on VSL and/or CVs

In recent decades, several measures have been proposed to prevent or delay the formation of congestion and improve traffic efficiency in bottleneck areas. These measures include VSL (Smulders, 1992), ramp metering (Papageorgiou et al., 1991), and lane change advisories (Park and Smith, 2012), etc. The principle of VSL is to set speed limits upstream of the bottleneck to slow down traffic and reduce the flow into the bottleneck to dissipate the existing queue and prevent future congestion. VSL control strategies can be classified into two primary categories: reactive rule-based approaches and proactive approaches (Khondaker and Kattan, 2015). Initially, VSL employed simple reactive rule-based logic, where real-time VSL control signals were modified based on predefined thresholds of traffic flow, occupancy, or mean speed. The main goal of these approaches was to enhance safety (Zackor, 1991; Smulders, 1992; Rämä, 1999). However, recent VSL research has predominantly focused on more sophisticated control logic that operates proactively, aiming to prevent traffic disruptions before they occur. These approaches are mainly designed to minimize the total time spent in the system (Hegyi et al., 2005; Hegyi and Hoogendoorn, 2010; Carlson et al., 2010). Both real-world applications and simulation experiments have confirmed that VSL systems offer significant benefits such as improved safety, enhanced traffic flow, and environmental advantages. VSL systems reduce speed differentials, synchronize driver behaviour, and prevent traffic breakdowns, leading to improved safety. They optimize traffic flow by resolving congestion and result in reduced fuel consumption and emissions, contributing to environmental benefits (Papageorgiou et al. (2008)).

2.3.1. Traditional variable speed limit

To achieve the advantages of VSL, researchers have explored various strategies for controllers and design variables. They have proposed different control methodologies, including feed-forward control, feedback control, and model predictive control. Hegyi et al. (2008) proposed SPECIALIST, a speed limit control algorithm based on shock wave theory. The approach uses a feed-forward control strategy and an open-loop optimization method to determine the control signals to the traffic process, including the activation and deactivation of VSL control, and suggested driving speeds. The SPECIALIST algorithm successfully addresses the shock wave issue on the A12 motorway in the Netherlands, as evidenced by simulations and real-world tests (Hegyi and Hoogendoorn, 2010). The parameters used in SPECIALIST have clear physical interpretations, making it suitable for real-world applications. This aspect enhances the understanding and implementation of the system. However, it is important to note that feed-forward control, as employed by SPECIALIST, may encounter challenges when adapting to changing traffic conditions and adjusting control signals promptly. This limitation suggests the need for further improvements to ensure the system can effectively respond to dynamic traffic situations and optimize its control signals in real-time. Papageorgiou et al. (1991) proposed ALINEA, a power local traffic-responsive strategy based on feedback structure. ALINEA is a simple, robust, flexible, and effective control system which has been confirmed by the application in a single on-ramp of the Boulevard Peripherique in Paris. ALINEA is simpler than other known algorithms and requires a minimal amount of real-time measurements (detectors). It is easily adjustable to particular traffic conditions because only one parameter is to be adjusted in a prescribed way. Inspired by ALINEA, Goñi-Ros et al. (2014) implemented the proportional feedback VSL control, which uses the concept of ”mainstream traffic flow control” to regulate the inflow into a sag bottleneck below the bottleneck capacity. The implemented feedback controller exhibited flexibility and adaptability, enabling it to handle diverse traffic scenarios and enhance roadway performance. The evaluation of this approach was conducted using simulations, with the total travel time serving as the performance metric. However, it should be noted that the longitudinal driving behaviour model used in the simulation lacked calibration and validation.

Another category of literature about VSL focuses on analyzing the parameters of VSL control and other factors that have an impact on the control effectiveness. Hellinga and Mandelzys (2011) used the PARAMICS microscopic traffic simulator to study the impact of driver compliance with VSL control signals. They designed several scenarios with different driver compliance and found that VSL operational impacts are sensitively and positively correlated with the level of driver compliance, while travel time

is negatively correlated with the level of compliance. They also point out that driver compliance levels are influenced by the used speed limits. These findings emphasize the interdependency between VSL impacts and driver compliance, concluding that designing a VSL control strategy cannot solely rely on speed limit enforcement. The conclusions of this study are supported by Habtemichael and de Picado Santos (2013), who conducted a study using the traffic simulation software VISSIM. They evaluated the effect of both traffic demand and driving compliance on the effectiveness of VSL control. They examined heavy congestion, light congestion, and uncongested traffic conditions, analyzing four levels of driver compliance within each condition: low, medium, high, and very high. The study found that higher speed limit compliance leads to increased safety benefits from VSL. Additionally, the safety benefits are more than four times greater in a high compliance scenario compared to a low compliance scenario. Another consideration is the control application location, which corresponds to the acceleration length of vehicles from the end of the VSL area to the entrance of the bottleneck. Martínez and Jin (2020) investigates the effect of applying VSL at different locations on congestion prevention. The location where the VSL is applied affects the acceleration length and thus the speed at which the vehicle reaches the bottleneck. They concluded that when reaching the bottleneck, only speeds greater than a specific speed, which is located on a congested branch of the downstream fundamental diagram and corresponds to a controlled traffic flow, can ensure an uncongested stationary traffic state and prevent capacity degradation. This specific speed is determined by the bounded acceleration rate at any location within the bottleneck. The optimal control application location is therefore equal to the acceleration length that achieves that specific speed. Assuming 100% compliance with the VSL, the researchers developed an equation to calculate the optimal control application location based on the applied speed limit in the case of a lane drop bottleneck and extended this approach to sag and tunnel bottlenecks.
Based on the above, it can be seen that VSL parameters and influencing factors on VSL control performance are highly interdependent, emphasizing the need to consider this relationship when designing a VSL strategy and improving its control effectiveness for specific scenarios.

2.3.2. CVs-based variable speed limit

In the near future, widespread adoption of CVs equipped with wireless communication is anticipated. These vehicles eliminate the necessity for costly roadside infrastructures, enhance the efficiency and accuracy of traffic data collection, and enable more flexible traffic control (Lee and Park, 2013; Khondaker and Kattan, 2015; Grumert and Tapani, 2017).
Several studies have been carried out to investigate the possible enhancement of traffic conditions using CVs-based VSL control.Grumert and Tapani (2012) incorporated cooperative systems into an existing VSL system and evaluated its performance using traffic simulation. The proposed cooperative VSL facilitates timely communication between vehicles and infrastructures by utilizing a roadside device to transmit speed limit signals to upstream vehicles, allowing them to adjust their speed earlier and smoothly. The simulation results demonstrate that the cooperative VSL reduces high acceleration and deceleration rates and exhibits a less varying speed pattern than the existing VSL. This indicates that the cooperative VSL promotes a more harmonized flow (more homogenous headways and decreased variance in speed), reducing adverse environmental impacts and lowering fuel consumption compared to the existing VSL. However, as with any new technology, real-world implementation poses significant challenges. One of the critical factors to consider is the MPR of CVs, which significantly affects control efficiency. Lee and Park (2013) utilized a VISSIM-based microscopic simulation model to assess the performance of VSL systems in the CVs environment. It is assumed that drivers equipped with CV technology can quickly respond to the provided speed limits. The driver compliance rate of all vehicles (both CVs and NCVs) to the speed limit is set to 20%. The study considers different MPR of CVs, including 20%, 40%, 80%, and 100%. Additionally, the performance of VSL without CVs (0% MPR) is evaluated for comparison. The simulation results show that the reduction in total travel time varied depending on the MPR of CVs. In the conventional VSL case (0% MPR), there is a 4.5% travel time saving compared to the scenario without VSL. However, as the MPR of CVs increased, the travel time savings also increased. With 100% MPR of CVs, a 12% travel time saving compared to the scenario without VSL is observed. Han et al. (2017) developed three comparison experiments with different MPR of CVs to explore and compare the effects of using CVs in VSL. The outcomes of all CV-based strategies demonstrate an overall enhancement in traffic conditions compared to Variable Message Sign-only control. These advantages include increased control efficiency by creating gaps ahead of CVs to alleviate queues, cost-effectiveness through the use of CVs or a single CV with a few VMSs,

and the ability of CVs to serve both traffic monitoring and control functions, streamlining implementation and reducing coordination delays.

Table 2.3: Reviewed literature about VSL control management

Paper	Traffic model	Objectives/Conclusions
Hegyi et al. (2008)	A feed-forward control strategy named SPECIALIST	Successfully address the shock wave issue on the A12 motorway in the Netherlands
Papageorgiou et al. (1991)	A feedback local traffic-responsive strategy named ALINEA	Effective application in a single on-ramp of the Boulevard Peripherique in Paris
Goñi-Ros et al. (2014)	A proportional feedback VSL control	Successfully regulate the inflow into a sag below the bottleneck capacity in simulations
Hellinga and Mandelzys (2011)	PARAMICS microscopic traffic simulator	Study the impact of driver compliance with VSL control signals
Habtemichael and de Picado Santos (2013)	Traffic simulation software VISSIM	Evaluate the effect of both traffic demand and driving compliance on the effectiveness of VSL control
Martínez and Jin (2020)	Simulation through building up the continuum car-following model with bounded acceleration	Investigate the effect of applying VSL at different locations on congestion prevention
Grumert and Tapani (2012)	Incorporated cooperative systems into an existing VSL system	A more harmonized flow, reducing adverse environmental impacts and lowering fuel consumption in comparison to the existing VSL
Lee and Park (2013)	VISSIM-based microscopic simulation	The reduction in total travel time varied depending on the MPR value, ranging from 7% for 0% MPR to 12% for 100% MPR.
Han et al. (2017)	Three comparison experiments with different MPR of CVs	An overall enhancement in traffic conditions compared to Variable Message Sign-only control

In summary, VSL has proven to be an effective control scheme in reducing congestion and improving traffic throughput. Integrating CV technology into VSL can further enhance its effectiveness by leveraging the power of in-time communication and data sharing. While previous research has explored the impact of MPR on overall control performance, there remain unresolved issues concerning the minimum MPR needed for effective control on specific road segments, such as sag and tunnel bottlenecks, and how MPR impacts other parameters of VSL control, such as the speed limit and the acceleration length. To fully understand the potential benefits of the CVs-based VSL, it is essential to fill these gaps.

2.4. Insights from literature review

In this thesis, we investigate the influence of MPR of CVs on preventing the capacity drop in sag and tunnel bottlenecks when applying VSL. We aim to contribute to the realization of a more robust and efficient traffic control system considering different MPR levels. A visual representation of the key insights gathered from the literature review for this study is presented through a conceptual framework.

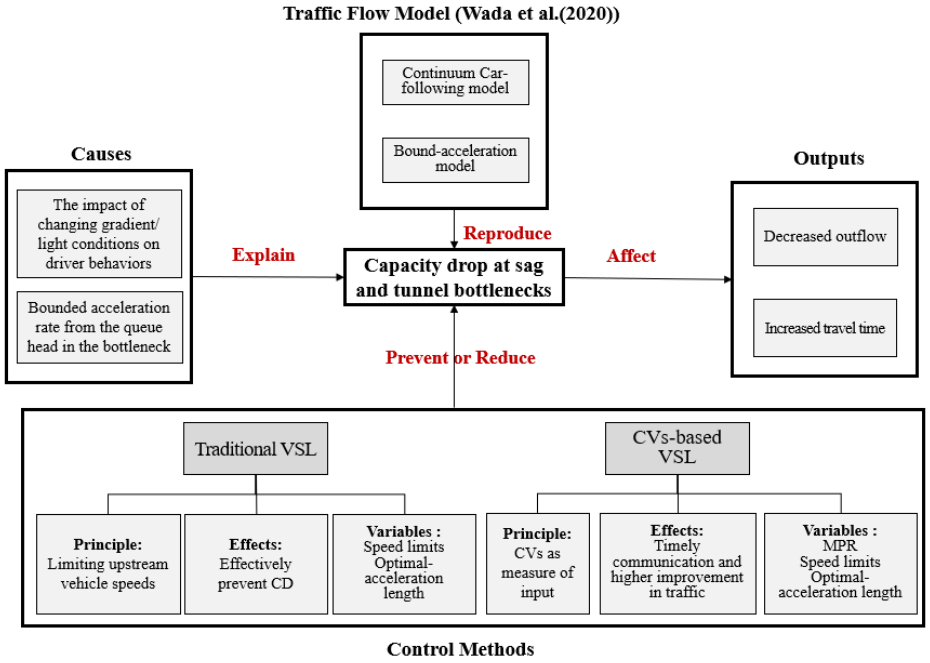

Figure 2.1: The conceptual framework for this research

At the core of this conceptual framework lies the main focus of this work: the capacity drop phenomenon observed at the sag and tunnel bottleneck. Four primary aspects must be taken into account to understand this complex issue. On the left side, root causes that contribute to the capacity drop in the single-lane sag and tunnel bottleneck are listed. The change in the gradient of the bottleneck and the darker lighting conditions cause vehicles to maintain longer headways than on normal roads, resulting in reduced road capacity (Koshi, 1985; Koshi et al., 1992). When traffic demand is higher than the reduced bottleneck capacity, congestion occurs. The acceleration rate after congestion is restricted by various factors such as vehicle mechanics, driver reactions, and road geometry. Even when there are no bottlenecks downstream, traffic flow is still influenced by the bounded acceleration behaviours of vehicles when they exit the queue (Jin, 2018). This flow is known as the queue discharge rate. It is lower than the bottleneck capacity and therefore the capacity drop phenomenon can be observed at the bottleneck. On the right side, the negative impact of capacity drop on traffic conditions can be assessed by comparing travel time and traffic flows at bottlenecks under the non-congested condition with those under capacity drop conditions.

At the lower part of the framework, strategies are classified into traditional VSL and CVs-based VSL and the principles and parameters are described. The traditional VSL prevents congestion at bottlenecks though intentionally slowing down the inflow upstream of the bottleneck by variable message signs on gantries. Researchers have analyzed some parameters that play a crucial role in the effectiveness of the control system. One parameter is the speed limit, which determines the maximum speed at which vehicles can travel through the controlled section of the road (i.e., the VSL zone). Another key parameter is the optimal acceleration length after passing the VSL zone. The study conducted by Martínez and Jin (2020) has provided valuable insights into the theory to determine the optimal acceleration length in traditional VSL, which serves as a valuable guide for this work. The incorporation of CVs into traditional VSL is expected to compensate for the limitations of traditional VSL, such as lack of flexibility and transmission delays between detector and controller. Through the use of telecommunication technology and CVs, traffic control can be implemented more proactively and timely. The influence of the MPR of CVs on overall traffic control performance has been confirmed in previous studies (Han et al., 2017; Lee and Park, 2013). These studies indicate that a higher MPR of CVs leads to better control effectiveness. However, its specific role and implications in the development of VSL remain unexplored. The interaction between the MPR of CVs and VSL parameters, namely the speed limit and the optimal acceleration length for this research, should be quantitatively studied. The control effectiveness in preventing capacity drop in specific traffic conditions can be achieved by adjusting VSL

parameters considering different MPRs of CVs.
Drawing upon the insights from the literature review, it has been determined that the traffic model proposed by Wada et al. (2020) is suited to model traffic conditions for this research context. The traffic flow model used consists of two key modules. One is the continuum car-following model, which is used to model the driving behaviour of following vehicles influenced by both the bottleneck geometry and vehicles in front. The other is a bounded acceleration model used to add constraints on vehicle acceleration. Although the model is based on a set of assumptions, the simulated traffic dynamics and capacity drop match the real-world observations well. The main benefit of this model is its simplicity (including limited parameters needed to be calibrated). Previously, Martínez and Jin (2020) has worked on the optimal location of VSL analytically based on an equivalent model proposed by Wada et al. (2020), which can be a reference for this thesis.

3

Research methodologies

This chapter provides a detailed description and mathematical formulation to explain the development of the traffic flow model and CVs-based VSL control strategy. Firstly, section 3.1 describes a continuum car-following model, including a bottleneck model, a bounded acceleration model and a car-following model, is borrowed from the literature to reproduce the vehicle behaviour in single-lane sag or tunnel bottlenecks (Wada et al., 2020). Section 3.2 introduces the implementation of a static open-loop VSL for mixed traffic environments with CVs in simulations. The speed limit calculation and theorems and formulas proposed by Martínez and Jin (2020) that determine the optimal acceleration length in alignment with the chosen speed limit of VSL assuming 100% compliance to VSL, are explained. Then, a method for introducing different levels of MPR of CVs into the simulated traffic is outlined. The selection of state variables is defined to represent the traffic states. Additionally, the study provides insight into the logic employed to adjust VSL parameters for different scenarios in simulation. This section also describes a method for quantitatively assessing the VSL control performance. Section 3.3 addresses the sources of uncertainties that may arise during the research process and presents strategies to consider them. Finally, the assumptions in the research methodology are outlined in section 3.4.

3.1. A continuum car-following model with bounded acceleration

The continuum car-following model with bounded acceleration proposed by Wada et al. (2020) is adopted. The model consists of three components. A bottleneck model represents the constraints on vehicle behaviour imposed by the bottleneck environment. A bounded acceleration model reflects limitations in the vehicle acceleration behaviour, due to physical constraints in vehicle mechanics, driver response, road geometry, etc. A continuum car-following model discrete real vehicles (i.e., vehicles with integral numbers) into imaginary vehicles (vehicles with non-integer numbers) to create a continuous traffic flow. The model captures the moving status of both real and imaginary vehicles at each time step.

3.1.1. The sag/tunnel bottleneck

A single-lane freeway stretch with a sag or tunnel bottleneck is considered. There are no on- or off-ramps in this stretch. The bottleneck is defined as the uphill section of the sag or the entire tunnel. Both upstream and downstream of the bottleneck are normal road sections. We set the starting point of the bottleneck to be the origin. The length of the bottleneck is denoted as L. Negative values of location (< 0) represent the upstream of the bottleneck, while values greater than L represent the downstream of the bottleneck. The capacity at the end of the sag/tunnel is regarded as bottleneck capacity. Vehicles travel in the direction of increasing values of location. The impact of characteristics of the bottleneck on vehicle behaviour is captured by assuming a linear increase in the time gap maintained by vehicles within the bottleneck (Jin, 2018). The time gap, also known as the ”minimum time gap”, refers to the minimum amount of time that should be maintained between a vehicle and the one directly ahead of it. It is a measure of the temporal spacing between vehicles. A shorter time gap means that vehicles are following each other more closely, while a longer time gap allows more space between vehicles.

On the other head, headways are the time intervals between the passage of successive vehicles, the inverse of which is the flow rate. The time gap for the studied road section is expressed as follows:

$$\tau(x) = \begin{cases} \tau_1 & \text{if } x \leq 0 \\ \tau_1 + \frac{\tau_2 - \tau_1}{L} x & \text{if } 0 < x \leq L \\ \tau_1 & \text{if } x > L \end{cases} \tag{3.1}$$

Where x is the location, $\tau(x)$ is the time gap at x, τ_1 is the time gap at the normal road section, and τ_2 is one at the end of the bottleneck, $\tau_1 < \tau_2$. The discontinuity of the time gap at the location $x = L$ denotes the assumption that there is no contains from downstream of the bottleneck. Fig. 3.1 shows a visualization of this assumption.

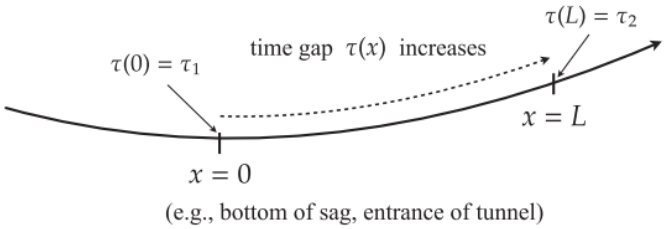

Figure 3.1: Illustration of a sag or tunnel bottleneck (Wada et al., 2020)

The time gap remains constant at τ_1 on both the upstream and downstream links, indicating no constraints on traffic flow from the downstream of the bottleneck. However, within the bottleneck, which spans from x = 0 to x = L, the time gap τ_x varies depending on location. This assumption is based on empirical observations. On an uphill section of the sag, drivers must exert more force on the pedal to accelerate, resulting in a larger gap between their vehicle and the one in front, compared to a level road at the same speed. Similarly, when driving through a tunnel, drivers tend to be more cautious due to lighting conditions, leading to a larger gap. In both cases, the time gap, namely the duration for a follower to cover the distance in front, increases continuously. Based on this, an inhomogeneous (i.e., location-dependent) triangular fundamental diagram for the modelled road section is proposed, see Eq. 3.2.

$$q(x,t) = \min\left\{ v_f k(x,t); \frac{1}{\tau(x)} \left(1 - \frac{k(x,t)}{k_j}\right) \right\}, \tag{3.2}$$

Where $q(x,t)$ is the flow rate, v_f is the free-flow speed, $k(x,t)$ is the density, k_j is the jam density.

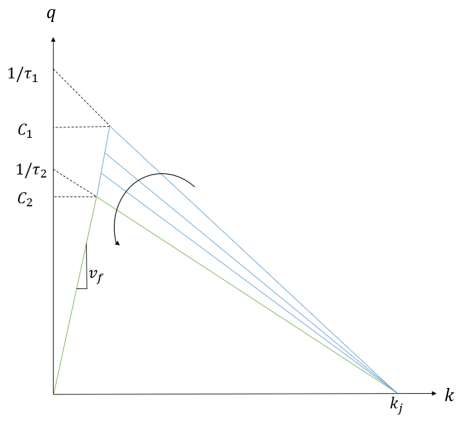

Figure 3.2: Fundamental diagrams: flow-density relation (Wada et al., 2020)

The road capacity also depends on the location:

$$C(x) = \frac{v_f k_j}{1 + v_f k_j \tau(x)} \tag{3.3}$$

We use C_1 to refer to the capacity of the normal section and the bottleneck entrance, and C_2 to refer to the bottleneck capacity before congestion (i.e., without capacity drop).

3.1.2. The bounded acceleration

Apart from the assumption of the inhomogeneous triangular fundamental diagram with the linear increase time gap within the bottleneck, another assumption is the bounded acceleration rate A_{max} of vehicles. Various models exist in the literature regarding constraints on bounded acceleration. They share some common properties, including (i) being non-negative (i.e., $A_{max}(x,v) \geq 0$); (ii) having a maximum start-up and being bounded (i.e., $A_{max}(x,v) \leq a_0 = A_{max}(x,0)$ (iii) being not increasing in speed (i.e., $\frac{\partial A_{max}(x,v)}{\partial v} \leq 0$) (Jin and Laval, 2018). The simplest model is the constant bounded acceleration (CBA) model with a constant value representing the bounded acceleration rate. More complex models, such as the Gipps model (Gipps, 1981) and the TWOPAS model (Allen et al., 2000), consider the relationship between speed and bounded acceleration rate. These different assumptions regarding bounded acceleration rate have an impact on vehicle driving behaviour and consequently affect the properties of capacity drop. This thesis assumes that the bounded acceleration rate follows the TWOPAS model, see Eq. 3.4.

$$\begin{aligned} &a(n) \leq A_{max}(x(n), v(n)) \\ &A_{\mathsf{max}}(x,v) = (a_0 - g\Phi(x)) \left(1 - \tfrac{v}{v_f}\right), \end{aligned} \tag{3.4}$$

Where $A_{\mathsf{max}}(x,v)$ is the bounded acceleration rate for the vehicle with the real-time speed v at x, $a(x,v)$ is the real-time acceleration rate at x, a_0 is maximum acceleration rate on a level road, g is gravitational acceleration, $\Phi(x)$ is the decimal grade at x.

3.1.3. Vehicle discretization and car-following behaviour

In their work, Jin and Laval (2018) introduced the bounded acceleration-LWR (BA-LWR) model. This BA-LWR model encompasses the LWR model, Lebacque's two-phase model, and the bounded acceleration version of Newell's car-following model, as follows.

$$\begin{aligned} &\tfrac{\partial k}{\partial t} + \tfrac{\partial (kv)}{\partial x} = 0 \\ &\tfrac{\partial v}{\partial t} + v\tfrac{\partial v}{\partial x} = \mathsf{min}\left\{A_{max}(x,v), \tfrac{V(x,k)-v}{\epsilon}\right\}, \end{aligned} \tag{3.5}$$

Where $V(x,k)$ is the speed-density fundamental diagram, ∂ is an operational symbol representing partial derivatives, $\epsilon = lim_{\Delta t \to 0+}\Delta t$ is a hyperreal infinitesimal number.
By solving the BA-LWR model with the inhomogeneous fundamental diagram of sag/tunnel bottlenecks in Lagrangian coordinates, as expressed in Eq. 3.2, the BA-LWR model can be transformed into a continuum car-following model with bounded acceleration specifically for sag and tunnel bottlenecks. The continuum car-following model is a first-order model when vehicles are in equilibrium states and a second-order model when vehicles are in bounded acceleration states. It computes the position of both real and imaginary vehicles by considering their current speed and acceleration rate at each simulation time step. This update assumes the acceleration rate of vehicles remains constant within the simulation time step Δ_t. The discretized formulations are shown below:

$$\begin{aligned} &x(t+d_t, n) = x(t,n) + \mathsf{min}\{V(x, s(t,n)), v(t,n) + A_{max}(x,v)\Delta_t\}\Delta_t \\ &V(x, s(t,n)) = \mathsf{min}\left\{v_f, \tfrac{1}{\tau(x(t,n))}(s(t,n) - s_j)\right\} \\ &s(t,n) = x(t,n-1) - x(t,n) \\ &s_j = \tfrac{1}{k_j} \end{aligned} \tag{3.6}$$

Where $x(t,n)$ and $v(t,n)$ are the position and the speed of n^{th} vehicle at time t, Δ_t is the simulation time step, $s(t,n)$ is the spacing between n^{th} vehicle and $(n-1)^{th}$ vehicle, s_j is the jam spacing.
In the model, time is a continuum variable and discretized by Δ_t. The concept of imaginary vehicles is then employed to discrete real vehicles into the continuum flow of imaginary vehicles by Δ_n. Traffic flow equations, including the conservation equation (Lighthill and Whitham, 1955) and the fundamental diagram, are typically formulated using aggregated variables that treat the movement of vehicles as a fluid. These equations are formulated in Eulerian coordinates, considering time and space as the coordinates. However, in this research, the traffic is modelled in Lagrangian coordinates, where time and vehicles serve as the coordinates. To ensure that the Lagrangian formulation is consistent with the Eulerian formulation, developing a continuum model in the Lagrangian framework is necessary. The additional imaginary vehicles introduced by discretization behave like real vehicles they represent, which

ensures accurate propagation of information among vehicles and eliminates the numerical viscosity (Wada et al., 2020). In Fig. 3.3, solid lines indicate real vehicles and dashed lines indicate imaginary vehicles introduced. The horizontal arrow indicates the direction of flow. The motion status of real and imaginary vehicles is then updated simultaneously at each time step.

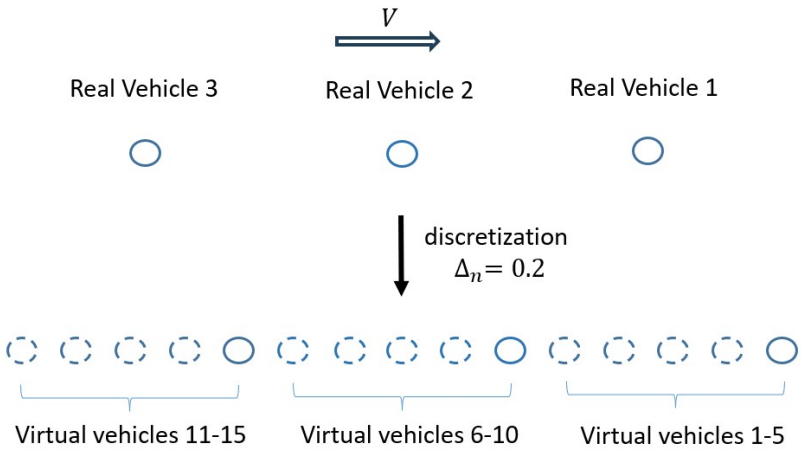

Figure 3.3: Discretization of vehicles

In order to satisfy the collision-free property (Wada et al., 2020; Jin, 2016), the appropriate discretized units Δ_t and Δ_n should satisfy the formula:

$$\frac{d_t}{d_n} \leq \tau_1 \tag{3.7}$$

3.2. An open-loop VSL for mixed traffic environments with CVs

This section introduces a strategy for implementing VSL control on CVs in a mixed traffic environment where both NCVs and CVs coexist. The goal is to adjust VSL parameters to prevent the capacity drop in sag and tunnel bottlenecks, considering different MPR of CVs. The approach assumes that the inflow entering the network cannot be influenced by any control measures. Thus, when the demand is higher than the bottleneck capacity, we limit the flow entering the bottleneck by limiting the speed of CVs at specific locations upstream of the bottleneck. Existing congestion within the bottleneck can be solved by the gap created by lowering speed, and possible congestion caused by high demand can be prevented meanwhile. When MPR is 100%, mathematical formulas proposed by Martínez and Jin (2020) are used to calculate the minimal required acceleration length to prevent the capacity drop in sag/tunnel bottlenecks for the specific speed limit. To prevent queues created by speed limits in the VSL zone from spilling back and blocking other upstream on- and off-ramps, it is expected to position the VSL zone as close as possible to the bottleneck. The optimum acceleration length is determined to be the shortest acceleration length that still prevents capacity drop. The research aims to identify the minimum conditions of MPR of CVs for formulas by Martínez and Jin (2020) to hold and suggests the determination of the speed limit and acceleration length when implementing VSL in CVs environment to prevent capacity drop and improve the traffic flow.

3.2.1. Key parameters of VSL: speed Limit and optimal acceleration length.

This section presents the method obtained from the literature for determining the speed limit range and optimal acceleration length specifically for a given speed limit in VSL. The speed limit range is determined considering the fundamental diagram and road capacity before and after capacity drop occurrence. For 100% MPR of CVs, the optimal acceleration length is calculated using the formulas proposed by Martínez and Jin (2020), considering factors like the speed limit, bottleneck geometry, jam density, and bounded acceleration rate for vehicles. For different MPR other than 100%, determining the optimal acceleration for a specific speed limit is expected to be the outcome of this study.

The speed limit range

The application of the speed limit serves the purpose of regulating traffic flow into a bottleneck by adjusting the speed upstream of the bottleneck. See Fig. 3.4, by implementing a speed limit VSL, a specific density k_{VSL} can be achieved in the VSL zone, thereby the controlled inflow C_{VSL} is achieved. According to the law of conservation, the inflow into the bottleneck equals the outflow at the end of the bottleneck when no vertex within the network creates or stores flows. To prevent congestion, the maximal speed limit should be set to ensure that the inflow does not exceed the bottleneck capacity. On the other hand, the minimum speed limit should be established to maintain the inflow above the dropped capacity of the bottleneck to avoid even lower flows after control.

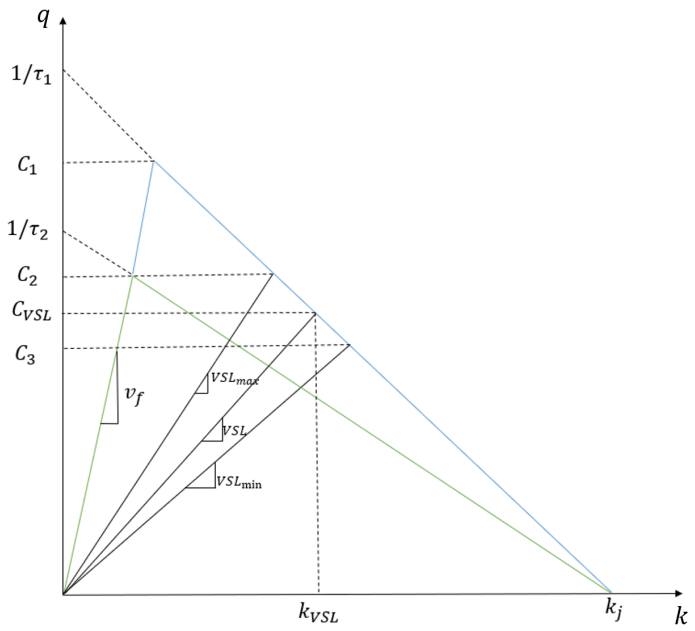

Figure 3.4: The speed limit range and associated flow rate

Assuming that the relationship between velocity and density described in the fundamental diagram is not affected by any control strategy, the maximum speed limit VSL_{max} can be calculated by Eq. 3.8.

$$VSL_{\text{max}} = \frac{v_f}{v_f k_j(\tau_2-\tau_1)+1} \tag{3.8}$$

The minimum speed limit VSL_{min} can be calculated by Eq. 3.9.

$$VSL_{\text{min}} = \frac{C_3}{k_j(1-\tau_1 C_3)} \tag{3.9}$$

Where C_3 represents the converged queue discharge rate when the capacity drop occurs at the bottleneck. This value can be calculated numerically from formulas proposed by Jin (2018). To avoid using a numerical solver, this value is obtained through simulations. In the case where no control management is applied and the capacity drop is observed, the converged traffic flow at the end of the bottleneck is the dropped capacity.
The controlled inflow C_{VSL} when applying a speed limit VSL can be calculated by:

$$C_{VSL} = \frac{k_j VSL}{k_j \tau_1 VSL+1} = \left(\tau_1 + \frac{1}{k_j VSL}\right)^{-1} \tag{3.10}$$

Optimal acceleration length

In stationary traffic, where traffic flow remains constant over time, speed and density can vary spatially. Two types of stationary states can be observed: bounded acceleration stationary states and equilibrium stationary states, which can be either congested or uncongested. (Martínez and Jin, 2020) proposed Theorem 1, that is, to avoid the capacity drop, the speed after vehicles exit the VSL zone should be determined based on bounded acceleration rather than relying on equilibrium stationary states before

returning to free flow speed. This constraint on the traffic state beyond the VSL zone can be translated into a requirement for the speeds at the entrance and end of the bottleneck. Specifically, it is important to ensure that the speed at the entrance to the bottleneck is at least equal to the imposed speed limit (i.e., $v_*(0) \geq VSL$) and that the speed at the end of the bottleneck is at least equal to the speed v_2 in Fig 3.5, which corresponds to the speed on the congested branch of the downstream fundamental diagram and for the controlled traffic flow C_{VSL} (i.e., $v_*(x = L) \geq v_2$) (Martínez and Jin, 2020). The required distance between the end of the VSL zone and the end of the bottleneck to prevent capacity drop is called critical length. Depending on the downstream congested speed, v_2, and the bounded acceleration model, the critical length may be longer than the minimal (optimal) acceleration length to prevent capacity drop.

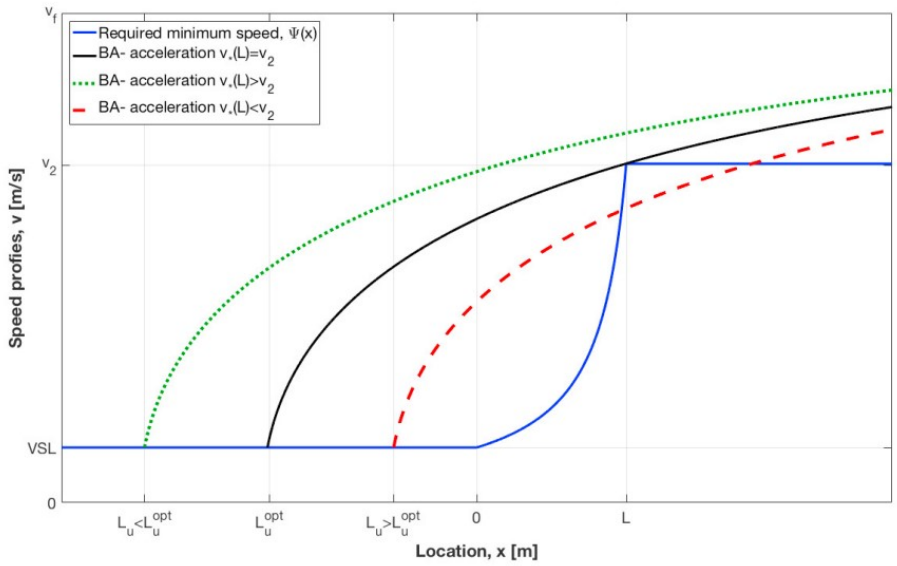

Figure 3.5: Illustration on the required speed at each location. The dashed-red speed profile is unfeasible, while dotted-green is feasible but not optimal. Only when $v_*(x = L) = v_2$, the control is implemented at the optimal application area, i.e. black speed profile.(Martínez and Jin, 2018)

These constraints are formulated mathematically by Martínez and Jin (2020), assuming all vehicles comply with the traffic control. Eq. 3.11 is based on Martínez and Jin (2018) for sag and tunnel bottlenecks. For a given speed limit VSL, the end location of the VSL zone is $-L_a$ and the acceleration distance from the end of the VSL zone to the entrance of the bottleneck is defined as $|L_a|$. To ensure that the mainline queue does not block other upstream on/off ramps, the shortest acceleration length is preferred, namely the maximal value of $-L_a$.

$$\begin{aligned} &\max_{L_a} L_a \\ &\text{s.t. } v(x)\frac{\partial v(x)}{\partial x} = A_{max}(x, v) \\ &v(L_a) = VSL \\ &v(L) \geq v_2 = \frac{VSL}{k_j \, \text{VSL}(\tau_1 - \tau_2) + 1} \\ &L_a \leq 0 \end{aligned} \tag{3.11}$$

By solving these formulas, the obtained acceleration length can ensure maintain desired traffic conditions and prevent capacity drop. By solving the formula, for lower speed limits the target speed v_2 is much lower and can be reached with a shorter distance. In contrast, for higher speed limits, the target speed v_2 increases and a longer distance is required, which is contrary to popular belief (Carlson et al., 2010; Lu et al., 2011). From Theorem 1 justified in the work done by Martínez and Jin (2020), it can be concluded that the minimum theoretical critical length is the zone where the time gap is increasing, i.e. the bottleneck length. Since we assume all CVs obey VSL, these formulations can be used to determine the optimal acceleration length for a specific speed limit when the MPR is 100%. However, when the MPR of CVs is less than 100%, it needs to be verified whether the Eq. 3.11 is still applicable.

3.2.2. Implementation and evaluation of VSL for CVs

To divide the vehicle platoon into CVs and NCVs, we utilize a randomized positioning mechanism while adhering to the predetermined MPR of CVs. This allows for a more realistic and diverse distribution of CVs within the platoon. After that, we develop strategies to implement VSL control for CVs, encompassing the adjustment and transmission of the driving instructions and the adaptation of the driving behaviour of CVs in response. Once the road traffic modelling and the implementation of the VSL system is completed, the design of scenarios and simulation tests are carried out. The method to determine various parameters in each scenario is introduced. To assess the performance of the VSL, we calculate the real-time traffic flow at the end of the bottleneck (i.e., the queue discharge rate) and compare the travel time in different scenarios. To achieve the result of preventing capacity drop in simulations, we devised approaches for adjusting the VSL parameters iteratively based on the simulation results.

Vehicle classification

Traffic in different scenarios contains different MPR of CVs. To achieve this, a percentage of vehicles, namely the MPR of the CVs, is randomly chosen from all real vehicles to act as CVs in the simulation. After the identification of CVs, both the CVs and NCVs are discretized using the same unit, creating corresponding virtual vehicles. Importantly, this discretization does not change their properties, i.e., the discretization of a CV is CVs and the discretization of an NCV is NCVs, see Fig. 3.6.

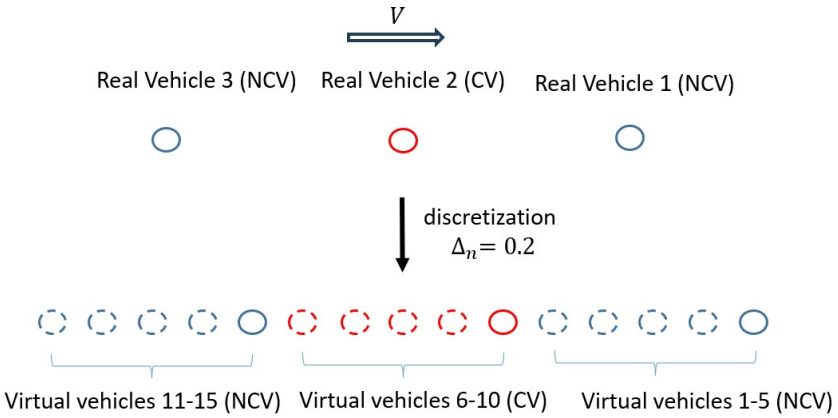

Figure 3.6: Visualization of discrete traffic with 33.3% MPR of CVs

Implementation of VSL and its impacts on traffic

Once the bottleneck traffic environment with a mixture of CVs and NCVs is established, the next step is to implement VSL, see Fig.3.7. VSL is activated when there is high demand upstream of the bottleneck (higher than the bottleneck capacity) detected by traffic monitoring devices. Then, the appropriate speed limit and corresponding optimal acceleration length are determined by the method which will be explained in the next section. The speed limit information is transmitted as the speed command to the CVs located at specific positions upstream of the bottleneck. When these CVs enter the VSL zone, their speed is assumed to immediately drop to the speed limit, without considering any deceleration time. Meanwhile, these CVs are provided with information about the optimal acceleration length, guiding them to start accelerating at the right location. The dashed line in Fig.3.7 means the location of the acceleration zone is not fixed for different scenarios. Implementing VSL can prevent congestion within a bottleneck but lead to new congestion in the VSL zone. However, due to the higher queue discharge rate in the VSL zone compared to the bottleneck, overall traffic flow is expected to improve. NCVs are not directly controlled by VSL. They adapt their driving behaviour based on the car-following behaviour described by Eq. 3.6.

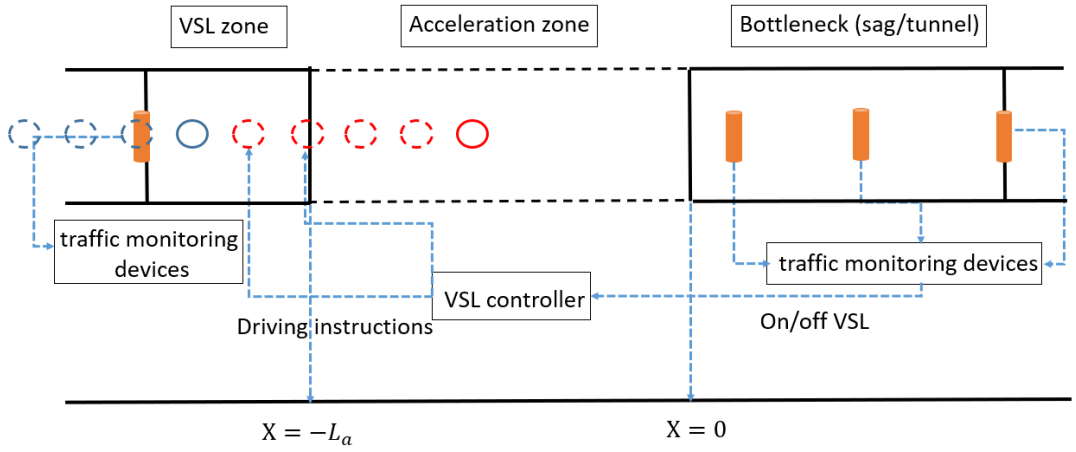

Figure 3.7: Visualization of VSL control system

The choice of appropriate VSL parameters enables effective prevention of capacity drop in both cases where the leading vehicle is a CV or an NCV. When the leading vehicle is a CV, it is controlled by VSL and a smooth flow without congestion is achieved. On the other hand, if the lead vehicle is an NCV, during periods of high demand, congestion will be caused by the platoon from the leading vehicle to the first CV (excluding the CV itself) within the bottleneck. However, this congestion will be resolved shortly due to the gap created by the speed limit imposed on the first CV.

Determination of VSL parameters considering MPR of CVs

To prevent capacity drop while maximising the throughput at sag/tunnel bottlenecks, this section explains the method to determine the appropriate speed limit and corresponding optimal acceleration length of VSL for scenarios with different MPR of CVs.

A higher speed limit means higher outflows at the end of the bottleneck when no congestion occurs. Therefore, we try to find the maximum speed limit that can prevent the capacity drop in the case where the MPR of CVs and acceleration length are predetermined. To realize this, an iterative approach is employed. At first, the maximum speed limit VSL_{max} is tested, and if it results in capacity drop, the minimum speed limit VSL_{min} is tested. If capacity drop still occurs, it is concluded that VSL is not feasible to prevent capacity drop in that particular case. If the capacity drop is prevented, a dichotomy method is used to narrow down the effective speed limit interval. By continuously observing the simulation results and reducing the effective speed limit interval until the length of the interval is less than $0.05km/h$, a maximum speed limit that can prevent capacity drop is eventually found.

For a specific speed limit, the optimum acceleration length can be directly calculated using Eq. 3.11 in the case of 100% MPR. However, in the case of lower MPR, the same parameters of VSL may not prevent the capacity drop. According to the findings from Martínez and Jin (2020), the speed of vehicles exiting the controlled area should be determined based on the bounded acceleration state to prevent capacity drop. Therefore, we proactively adapt the acceleration length to ensure that vehicles drive in the bounded acceleration state. A method which is similar to the one used to determine the speed limit is employed to gradually reduce the interval of feasible acceleration length that prevents capacity drop. When this interval becomes less than $50m$, it is regarded that the optimal acceleration length that prevents capacity drop has been identified.

Evaluation of VSL control performance

The traffic flow rate at the end of the bottleneck serves as an indicator to assess the traffic conditions and the effectiveness of the VSL. To evaluate the real-time flow rate, we assume there are traffic monitoring devices equipped at the end of the bottleneck, recording the passing time for individual vehicles. This study does not account for potential measurement errors that may arise from traffic monitoring systems. By analyzing the temporal spacing between consecutive real vehicle passages, we can calculate the real-time traffic flow rate $q_{t(n,L),L}$, which is derived by taking the reciprocal of the time headway between successive vehicle passages:

$$q_{L,T(n)} = 3600/(T(n-1) - T(n)) \tag{3.12}$$

Where $T(n)$ refers to the time when the n^{th} real vehicle passes the end of bottleneck. In the simulation where time is discretized, the positions of vehicles are also discretized. The method utilized to determine the $T(L)$ is identifying the adjacent positions of the bottleneck end and then using the interpolation to determine an approximation value of $T(L)$. By normalizing the queue discharge flow rate $q_{L,T(n)}$ with the bottleneck capacity C_2, we obtain the road capacity utilization.
Furthermore, we analyze the influence of VSL on travel time, which directly reflects the effectiveness of VSL control. By comparing vehicle travel times in the base case without control to the controlled case where the capacity drop is prevented, we assess the impact on both individual vehicle travel times and average travel times. To capture the overall influence of VSL, travel times are measured for the entire road section. It is ensured that the measured vehicles start at free-flowing speeds and return to free-flowing speeds.

3.3. Simulation scenarios

The research comprises five scenarios aimed at quantifying the relationship between the MPR of CVs, the speed limit, and the optimal acceleration length. Each scenario involves many cases. The underlying principle of designing scenarios for simulations is to fix two variables and adjust the third variable according to the simulation results.
Scenario 1 is used to evaluate the bottleneck capacity and observe the capacity drop phenomenon. Two base cases are conducted without any control measures: the first case is simulated with low demand (D_1), while the second case uses high demand (D_2). These cases also serve as a baseline for analyzing the effectiveness of the VSL control. Scenario 2 is used to test the validity of the theorems and formulas proposed by Martínez and Jin (2020) in the presence of varying MPR of CVs. These theorems and formulas, specifically Eq. 3.11, calculate the optimal acceleration length required to prevent capacity drop for each speed limit. In scenario 2, the VSL control is implemented using the maximum speed limit (VSL_{max}) and the corresponding optimal acceleration length calculated by the proposed formulas. The objective is to identify the minimum MPR of CVs necessary to effectively prevent capacity drop when applying the VSL control. Various cases are examined, each representing different MPR levels of CVs, ranging from 100% to 0%. Scenario 3 establishes the critical acceleration length needed for cases where the MPR of CVs falls below the threshold determined in Scenario 2. In scenario 3, the cases conducted have MPRs of CVs lower than the minimum MPR identified in scenario 2. The acceleration length for each case is increased and tested in simulations to identify the minimum acceleration length necessary for preventing capacity drop. In scenario 4, the aim is to determine the maximum speed limit that can effectively prevent capacity drop for cases with different MPR of CVs in the absence of an acceleration zone. The acceleration length ($|L_a|$) is held constant at $0m$. By varying the speed limit in each case and observing the simulation results, scenario 4 seeks to identify the upper limit of the speed limit range that can prevent capacity drop. Building on the simulation results obtained from scenarios 3 and 4, scenario 5 focuses on determining the optimal acceleration length for different speed limits in cases with varying MPR of CVs. The MPR levels considered in this scenario are 100%, 75%, 50%, and 25%. The objective of scenario 5 is to identify the ideal combination of acceleration length and speed limit that prevent capacity drop while taking into account the specific MPR of CVs.
These scenarios provide a comprehensive understanding of the impact of MPR of CVs on the speed limit and acceleration length of VSL in capacity drop prevention and traffic flow optimization. The overview of scenarios simulated in this research is listed in Table 3.1.

Table 3.1: Summary of simulation scenarios

Scenario	Purpose
1	Two base cases without any VSL control: one with low demand and the other with high demand
2	Determine the minimum MPR of CVs for which the conclusions by Martínez and Jin (2020) holds
3	Determine the optimal acceleration length for cases where the MPR of CVs falls below the threshold
4	Determine the maximal speed limit for different MPR of CVs without acceleration length
5	Determine the optimal combination of the speed limit and acceleration length for 100%, 75%, 50%, and 25% MPR of CVs

3.4. Simulation uncertainties

In the section, several sources of uncertainties which affect simulation results are discussed. They arise from assumptions, traffic models, the VSL control strategy, and simulation methodologies. These uncertainties can impact the simulation results in different ways. Some of these uncertainties can be

quantified or mitigated, while others are inherent and cannot be precisely quantified. Numeric errors, stemming from time and vehicle discretization, are one source of uncertainty that can be managed through converged analysis. On the other hand, the random order of CVs within platoons introduces variability in traffic dynamics evolution. Considering the computational effort, five repeated simulations are required to account for this uncertainty.
The continuum car-following model used in this study discretizes time and vehicles to create a continuum traffic flow. To mitigate the influence of numerical errors, a convergence analysis is required. This analysis aims to determine the maximum discretization unit that can be used while maintaining consistent simulation results in the same scenario. The convergence analysis will be presented in Section 5.1. To consider the effects of all simulation parts which may introduce numerical errors through discretization, it is important to perform the convergence analysis after completing the VSL implementation in the traffic flow models in sag/tunnel bottlenecks. Since the order of CVs in the traffic can also affect the experimental results, an assumption of 100% MPR is made for the scenario used to conduct convergence analysis to avoid interference from different CV orders.
As mentioned above, time is divided into discrete time steps in the simulation, and as a result, the position of vehicles on the road is also discretized into separate points. It is not possible to directly obtain the time at which vehicles pass the end of the bottleneck. However, to monitor traffic changes and visualize the capacity drop, it is crucial to track real-time traffic flow at the end of the bottleneck. To address this challenge, we employ the interpolation technique. By determining the time when a vehicle passes two adjacent positions, one on the left and one on the right of the end of the bottleneck, we can estimate the approximate moment when the vehicle passes through the end of the bottleneck. This is a linear approximation, and it can also induce numerical errors, which are minimized by reducing Δ_t.
When considering a specific value of MPR, random positioning of CVs within the vehicle platoon affects the reliability of capacity drop prevention. To be specific, different simulation runs conducted for the same scenario may yield contrasting results. Some runs successfully prevent capacity drop, while others may not. To guarantee the robustness of the prevention of capacity drop by VSL with the predetermined parameters, it's necessary to conduct repeated simulations. Five repeated simulation runs are conducted for each scenario while maintaining consistent values for all parameters. Conclusions regarding the feasibility of parameter values are drawn only if the prevention of capacity drops is successful in all simulation runs. During our analysis, it is observed that the timing of the flow drop varies across different simulation runs when capacity drops occur. To gain a better understanding of these divergent outcomes, a comparative analysis of the simulation results from each run is performed. The objective is to gain insights into the complex dynamics of capacity drops and further improve the understanding of their underlying causes.

3.5. Summary of assumptions

It is important to acknowledge that any modelling or simulation work involves making certain assumptions to simplify the problem and make it more tractable. Assumptions for each research step in this research have been mentioned previously. Here, an overview of the main assumptions made is provided.

1. The continuum car-following model with bounded acceleration
    - I Sag/tunnel bottleneck model
        - i. A linear increase of the time gap within bottleneck, see Eq. 3.1
        - ii. An inhomogeneous triangular fundamental diagram, see Eq. 3.2
    - II TWOPAS BA model: bounded acceleration rate, see Eq.3.4
    - III Car-following model
        - i. Newell's simplified car-following model
        - ii. Constant vehicle acceleration rate within a simulation time step
2. VSL control strategy
    - I The inflow into the network will not be affected by any control strategies
    - II The relationship in the fundamental diagram will not be affected by any control strategies CVs 100% comply with the instructions from VSL

III Traffic monitoring systems capture the driving behaviour of individual vehicles
IV The speed of the CV is reduced to the speed limit immediately after entering the VSL zone,

3. Initial conditions

I Constant headway in the initialization
II The starting position of the lead vehicle
III The network is initially empty

4. Boundary conditions: constant demand over the simulation time

4

Simulation results

This section presents an overview of the simulation design and results. The parameters of the continuum car-following model obtain from Jin (2018) are listed. Two demand levels are introduced to observe the capacity drop phenomenon. The section also introduces the initialization of the simulation. Furthermore, the research describes five simulation scenarios aimed at quantifying the relationship between the MPR of CVs, speed limits, and optimal acceleration lengths.

4.1. Simulation setup

The parameters of the continuum car-following model requires calibration. These parameters include the length of the bottleneck denoted as L, the time gaps at the entrance and end of the bottleneck represented by τ_1 and τ_2 respectively, the free-flow speed denoted as v_f, the jam density expressed as k_j, the maximum acceleration rate on a level road denoted as a_0, and the decimal grade $\phi(x)$, which reflects the gradient of the bottleneck. The values of calibrated parameters used in this thesis are obtained from Jin (2018). But $\Phi(x)$ is set to 0, which indicates a level tunnel is considered. The source of empirical data for calibration done in the work of Jin (2018) is collected at the Kobotonoke tunnel bottleneck in Japan (Koshi et al., 1992). Moreover, the capacity of both the normal road C_1 and the bottleneck end C_2 can be calculated using Eq. 3.3.

To simulate the traffic flow, two demand levels are introduced: D_1 and D_2, representing constant inflows into the road network. D_1 is set slightly below the bottleneck capacity. D_2 exceeds the bottleneck capacity (C_2), enabling the observation of the capacity drop phenomenon and its characteristics. The simulation involves a total of n_v real vehicles and the simulation time is set to t_f. The duration of the simulation ensures that the bottleneck reaches a final stationary flow rate in all cases. Furthermore, the length of the VSL zone, denoted as L_{VSL}, allows sufficient space for all vehicles to adjust their driving behaviours to drive at the imposed speed limit with the headway corresponding to the relationship of speed and headway depicted in the congested branch of the fundamental diagram.

In the initialization of the simulation, we assume that vehicles within the platoon are spread out with the same spacing. The initial distance between two imaginary vehicles denoted as h, is determined by the following equation:

$$h = (v_f d_n)/D \tag{4.1}$$

Due to the asymptotic shape of the TWOPAS model, when 100% MPR of CVs and maximal speed limit VSL_{max} is applied, the optimal acceleration length $|L_a|$ obtained from Eq. 3.11 tends towards infinity. Thus, the maximum speed limit from Eq. 3.8 is slightly rounded down to the first decimal to avoid the non-meaningful result. By substituting the values of parameters into Eq. 3.8, a maximum speed limit of $27.5km/h$ can be calculated.

Table 4.1: Parameters of the simulation (Koshi et al., 1992)

Parameter	Value	Unit
Free-flow speed, v_f	80	km/h
Jam density, k_j	140	veh/km
Maximum acceleration rate on a level road, a_0	0.407	veh/s^2
Decimal grade at x, $\phi(x)$	0	—
Bottleneck length, L	1.5	km
Time gap upstream to the bottleneck, τ_1	1.5	s
Highest time gap inside the bottleneck, τ_2	2.1	s
Capacity of the start of tunnel, C_1	2000	veh/h
Capacity of the end of tunnel, C_2	1500	veh/h
Low Demand, D_1	1480	veh/h
High Demand, D_2	1725	veh/h
The number of simulated real vehicles, n_v	450/600	veh
The simulated time, t_f	1200	s
The length of VSL zone, L_{VSL}	100	m

4.2. Convergence analysis of discretizations

As mentioned in Section 3.4.1, the discretization method employed for simulating the driving behaviour of imaginary vehicles at each time step will introduce numerical errors. To ensure the reliability of the simulation results, a convergence analysis is performed to identify the maximum discretization units for achieving consistent outcomes in the same scenario. The discretization of vehicles (Δ_n) and time (Δ_t) must adhere to the collision-free condition outlined in Eq. 3.7. Consequently, rather than directly modifying the values of Δ_n and Δ_t, the values of Δ_n and the ratio $\frac{\Delta_t}{\Delta_n}$ are adjusted across different simulation runs for the convergence analysis.

The convergence analysis focuses on a specific case with 100% in scenario 2. In this scenario, VSL control is applied to the traffic with 100% MPR of CVs, utilizing a maximum speed limit of VSL_{max} and an optimal acceleration length of $|L_a|$, which is calculated using Eq. 3.11 and results in $1140m$. The flow rate at the end of the bottleneck is selected as an indicator to assess the simulation results. The flow rates for each simulation run are calculated using Eq. 3.12 and recorded in Table 4.2. By comparing the flow rates obtained from each simulation run, the maximum discretization units at which the simulations result in a constant flow rate are identified.

Table 4.2: Flow rate [veh/h] and corresponding discretization in the numerical example

$\frac{\Delta_t}{\Delta_n}$	$\Delta_n = 1$	$\Delta_n = 0.5$	$\Delta_n = 0.25$	$\Delta_n = 0.1$	$\Delta_n = 0.02$
1.5	1390.5	1384.3	1381.5	1379.5	1378.4
1	1383.5	1386.5	1382.5	1379.8	1378.5
0.5	1397.9	1388.3	1383.3	1380.3	1378.5
0.25	1401.2	1389.2	1383.8	1380.4	1378.5
0.05	1478.8	1479.4	1478.8	1478.2	1478.2
0.02	1478.6	1478.3	1478.9	1478.2	1478.2

The simulation results demonstrate that different discretization units lead to varying inflow to the bottleneck in different simulation runs for the same scenario. While the capacity drop is expected to be prevented in this scenario, the flow rate theoretically from the speed limit and the predetermined fundamental diagram (see Eq. 3.2) is $1478.2veh/h$. When $\frac{\Delta_t}{\Delta_n} \geq 0.05$, the capacity drop can not be prevented and the resulting flow doesn't match the theoretical value. While the ratio $\frac{\Delta_t}{\Delta_n}$ is equal to or less than 0.05, the flow converges to a consistent value of $1478.2veh/h$ for different simulation runs, indicating successful prevention of capacity drop through VSL control as anticipated. On the other hand, a small value of Δ_n must be ensured to create a continuum traffic flow. To ensure a continuum traffic flow and minimize numerical errors while optimizing computational efficiency, a discretization value of $\Delta_n = 0.1$ and a ratio of $\frac{\Delta_t}{\Delta_n} = 0.05$ are selected for all simulations in this research. Using these discretised units and the parameters listed in Table 4.1, the average time required to run a $20mins$ simulation, using a Windows 10 laptop with a processor of 11^{th} Gen Intel(R) Core(TM) $i7-11800H$@$2.30GHz$ and the memory of $32.0GB$, is about 2 hours.

4.3. Scenario 1: two base cases without control

In scenario 1, two base cases are examined to understand the behaviour of uncontrolled traffic in the tunnel bottleneck. These cases represent two distinct traffic scenarios: non-congested and congested, which depend on the traffic demand. In case 1, the demand (referred to as D_1) is slightly below the capacity of the bottleneck. This results in smooth traffic flow without congestion. In case 2, the demand (referred to as D_2) is higher than the bottleneck capacity but lower than the normal road capacity. This leads to congestion within the bottleneck, causing a capacity drop phenomenon at the end of the bottleneck. The congestion then propagates upstream, affecting the upstream traffic. These base cases are crucial for evaluating the bottleneck capacity and serve as reference scenarios to assess the effectiveness of VSL control when it is implemented to mitigate congestion and prevent capacity drop.
The simulation results obtained in this study provide a representation of real vehicle movements, including detailed information about vehicle trajectories, speed profiles and the evolution of the normalized traffic flow rate at the end of the bottleneck. The analysis focuses on analyzing and comparing the driving behaviour within the bottleneck in two base cases, aiming to gain an understanding of the distinct traffic dynamics that emerge. In case 2, the occurrence of the capacity drop phenomenon is observed. The characteristics of the capacity drop, such as the duration of the transition period and the capacity drop ratio, are directly visualized in the evolution of the normalized traffic flow rate at the end of the bottleneck. The dropped bottleneck capacity after congestion is obtained and then utilized in the calculation of the lower bound of the speed limit range of VSL using Eq.3.9.

4.3.1. Case 1: no capacity drop with a low demand

The simulation results for case 1 are shown in Fig. 4.1. The black line in Fig. 4.1(a) indicates the bottleneck location.

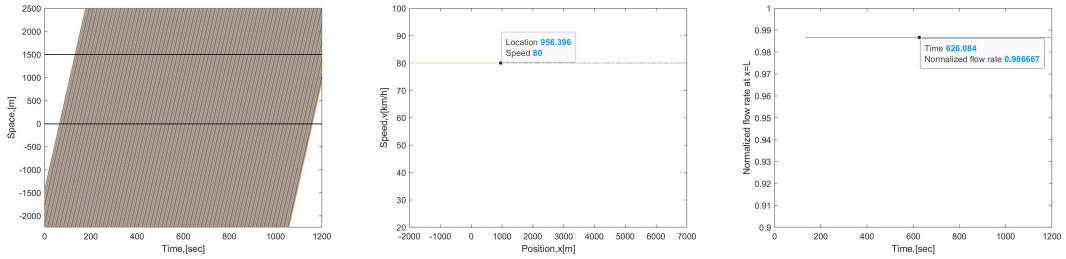

(a) Vehicle trajectories of real vehicles **(b)** Speed profile of real vehicles **(c)** Evolution of traffic flow rate at x=L

Figure 4.1: Numerical example for base case 1 with a low demand

Fig. 4.1 depicts the stationary traffic condition without congestion. In this situation, vehicles travel at their free-flow speed for the whole road section. The outflow rate at the end of the bottleneck matches the inflow rate into the network, namely the demand D_1.

4.3.2. Case 2: capacity drop with a high demand

The simulation results for case 2 with high demand D_2 are shown in Fig. 4.2.

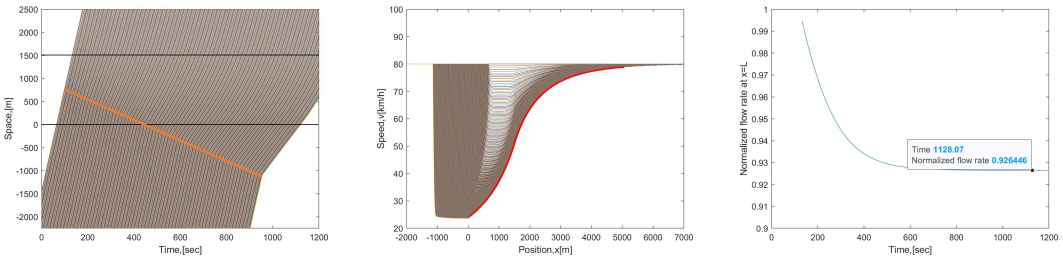

(a) Vehicle trajectories of real vehicles **(b)** Speed profile of real vehicles **(c)** Evolution of queue discharge flow rate at x=L

Figure 4.2: Numerical example for base case 2 with a high demand

It can be seen in Fig. 4.2(a)(b), vehicles experience a sudden drop in speed within the bottleneck. The road capacity in the bottleneck decreases linearly. As vehicles approach the bottleneck with high inflow, they reach a critical point where the capacity becomes lower than the inflow rate. At this point, vehicles experience an abrupt transition from the free-flow speed to the congested branch of the fundamental diagram, assuming no deceleration time. This speed change initiates in the second vehicle of the platoon and propagates to the upstream vehicles, one by one. This adaptation in driving behaviour corresponds to the onset and propagation of congestion, as indicated by the yellow line in Fig. 4.2(a). Subsequently, vehicles gradually accelerate from the front of the congested queue, but their acceleration rate is constrained by the bottleneck, resulting in a lower acceleration rate than the bounded acceleration rate. This equilibrium congested acceleration state continues until vehicles exit the bottleneck. Once outside the bottleneck, vehicles can accelerate at the bounded acceleration rate, eventually returning to the free-flow speed. Overall this entire process involves the transition from a free-flow stationary state to a congested stationary state, followed by a non-equilibrium bounded acceleration stationary state, before finally returning to the free-flow stationary state.
The speed profiles are plotted in Fig. 4.2(b), showing a convergence towards a stationary acceleration profile which is depicted by the red line. This observation is consistent with the results obtained from a calibrated first-order model and empirical data (Martínez and Jin, 2020). By comparing the evolution of the normalized flow rate at the end of the bottleneck in Fig. 4.1(c) and Fig. 4.2(c), the capacity drop is observed. The transition period from the start of congestion to the capacity drop stationary state is about $16mins$. The dropped bottleneck capacity after congestion C_3 is $1380veh/h$. This value obtained in the simulation is consistent with empirical data (Koshi et al., 1992; Wada et al., 2020). Using this value, the minimum speed limit calculated by Eq.3.9 is $23.2km/h$. Consequently, the range of the speed limit of VSL is from a minimum of $23.2km/h$ to a maximum of $27.5km/h$.

4.4. Scenario 2: determining the minimum MPR to have the highest flow

In scenario 2, the VSL control is applied with a fixed speed limit of $27.5km/h$ for all cases. The acceleration length from the end of the VSL zone to the bottleneck entrance is fixed to the value calculated using Eq.3.11, which is $1140m$. The MPR of CVs varies for different cases. Initially, a simulation is conducted with 100% MPR of CVs, aiming to prevent the capacity drop as suggested by Martínez and Jin (2020). The control performance of the VSL is evaluated based on the simulation results from this case. Subsequently, simulations are performed with 50%, 75%, 85%, and 95% MPR of CVs in sequence. However, in all these cases, the capacity drop phenomenon still occurs, as indicated in the results presented in Table 4.3.

Table 4.3: Summary of simulation results from scenario 2

Case	1	2	3	4	5
MPR	100%	95%	85%	75%	50%
Speed limit (km/h)	27.5				
Optimal acceleration length from 3.11 (m)	1140				
Flow rate at the bottleneck (veh/h)	1478.2	1380.6	1380.5	1380.6	1380.4
Prevention capacity drop or not	Yes	No	No	No	No

These simulations provide insights into the requirements for successful implementation of the VSL control strategy proposed by Martínez and Jin (2020) under different MPR of CVs conditions. It is concluded that based on research assumptions, achieving 100% MPR of CVs is necessary to effectively prevent the capacity drop in the tunnel bottleneck when using calculation formulas proposed by Martínez and Jin (2020) for deriving the acceleration length in VSL control.

4.4.1. Case 1: capacity drop prevention with 100% MPR of CVs

The simulation results for the case with 100%MPR of CVs are shown in Fig. 4.3. The green lines indicate the location of the VSL zone in this scenario, which is from $-1240m$ to $-1140m$.

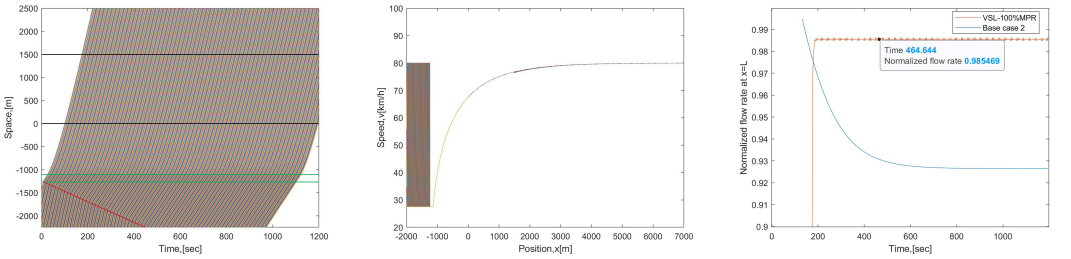

(a) Vehicle trajectories of real vehicles **(b)** Speed profile of real vehicles **(c)** Comparison of traffic flow rate at x=L

Figure 4.3: Numerical example for case 1 with 100% MPR

In this case, all vehicles are CVs, and the VSL is applied. The speed of the leading vehicle is constrained within the VSL zone, even though it will not be stuck in congestion. The driving behaviour of the following vehicles is influenced by both the VSL and the driving behaviour of the preceding vehicles. The VSL control is assumed to be activated immediately at the beginning of the simulation when the demand input is D_2, which exceeds the bottleneck capacity. As vehicles enter the VSL zone, their speed is reduced to the predetermined speed limit of $27.5km/h$ without deceleration time. The flow within the VSL zone is then regulated to match the flow on the congested branch of the normal road fundamental diagram associated with the defined VSL speed. This flow is slightly below the bottleneck capacity. Vehicles within the VSL zone experience congestion, which gradually propagates upstream of the VSL zone along the red line as shown in Fig 4.3(a).
Once vehicles pass through the VSL zone, they accelerate one by one at a bounded acceleration rate until reaching the free-flow speed. The traffic becomes stable as the speed and the spacing between vehicles increase simultaneously. The speed profiles of all vehicles, depicted in Fig.4.3(b), show overlapping acceleration profiles. No congestion occurs within the bottleneck. The outflow from the bottleneck matches the inflow into the bottleneck, which is also the outflow from the VSL zone. This outflow rate is higher than the observed dropped capacity C_3 in base case 2. As a result, the capacity drop at the end of the bottleneck is effectively prevented.

The improvement of travel time

In section 4.3.2, it is observed that when congestion occurs, the acceleration profiles of vehicles gradually converge, resulting in a stationary queue discharge rate at the end of the bottleneck. The transition period for reaching the capacity drop stationary state is $16mins$. The impact of VSL on vehicle travel times compared to the uncontrolled scenario is assessed by analyzing and comparing travel times across three cases: base cases 1 and 2 in scenario 1 without VSL, and case 1 in scenario 2 with VSL applied to 100% MPR of CVs. The analysis considers both the travel times of individual real vehicles that reached the end of the bottleneck before and after the transition period and the average travel times of all simulated vehicles across the different cases.
The road section for evaluating travel time spans from $-3000m$ to $5000m$, which is indicated as the grey line in Fig 4.4. In all cases, vehicles start with the free-flow speed and eventually return to the free-flow speed after undergoing a series of speed changes when driving along this road section. It is important to note that as the speed approaches the free-flow speed, the bounded acceleration rate determined by the TWOPAS model becomes infinitely small. To prevent the selected road section from becoming excessively long, we consider the speed to have returned to the free-flow speed when it reaches 98.5% of the free-flow speed. Fig 4.4 provides a graphical representation of the speed profiles for the 400^{th}

vehicle in base case 2 and case 1 in scenario 2. This visualization illustrates the dynamics of speed changes during the capacity drop phenomenon and its mitigation through the implementation of VSL control. It can be observed, for the 400^{th} vehicle, in the congestion case (base case 2), the dropped speed after congestion is lower than the speed limit applied in the VSL control case.

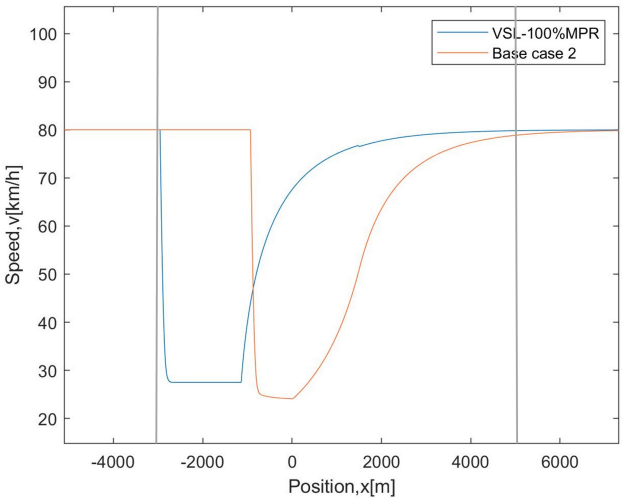

Figure 4.4: Comparison of speed profiles of the 400^{th} vehicle

The travel times for individual vehicles and average travel time for all simulated vehicles in three cases are presented in Table 4.4.

Table 4.4: Travel time comparison in three cases

Vehicle number	Arrive time at the bottleneck end $T(n)$	Travel time, (s)			Improvement	
		Without VSL		VSL		
		Low demand	High demand	High demand	Difference	Percentage (compare to the travel time in base case 2)
100^{th}	Within the transition period	360	419.5	440	-20.5	-5%
200^{th}			470.6	475.0	-4.4	-0.9%
250^{th}			495.8	492.4	3.4	0.6%
300^{th}	After the transition period		521.0	509.7	11.3	2%
400^{th}			586.0	545.0	41	7%
Average of all 450 vehicles	/		483.4	484.5	-1.1	-0.2%
Average of all 600 vehicles	/		521.2	502.3	20	4%

The improvement in travel time highlights the beneficial effect of VSL implementation on vehicles passing the selected road section. Vehicles located at the front of the platoon (e.g., the 100^{th} and 200^{th} vehicles) experience longer travel times when VSL is applied. These unexpected situations can be explained that the speed which is corresponding to the congested branch of the fundamental diagram is higher than the maximal speed limit of VSL. On the other hand, vehicles located at the back of the queue (e.g., the 250^{th}, 300^{th}, and 400^{th} vehicles) benefit from the VSL implementation, as the speed limit set by VSL is higher than their speeds after congestion. Furthermore, the implementation of VSL allows vehicles to accelerate at the bounded acceleration rate after exiting the VSL zone, which is higher than the acceleration rate experienced during the congestion stationary state, as depicted in Fig 4.4. The advantages of VSL in reducing travel time are more pronounced for vehicles positioned further back in the queue. For instance, the ratio of travel time reduction for the 400^{th} vehicle is higher than that for the 300^{th} vehicle.

To ensure overall improved traffic conditions in terms of average travel time, it is recommended to apply VSL when the number of vehicles within the network exceeds a specific threshold or when high demand persists over a significant period in real-world scenarios. Otherwise, vehicles may experience an average longer travel time compared to the uncontrolled scenario. The simulation results provide evidence of the impact of VSL in different scenarios. In the case where there are 450 vehicles, the implementation of VSL results in increased average travel time. However, when the total number of vehicles entering the network increases to 600, applying VSL leads to a reduction in average travel time.

4.4.2. Case 2: capacity drop with 95% MPR of CVs

The effectiveness of the VSL strategy proposed by Martínez and Jin (2020) in preventing the capacity drop is tested with different MPR values of CVs, including 50%, 75%, 85%, and 95%. However, it is unexpected that even with a 95% MPR of CVs, the capacity drop could not be prevented, as depicted in the corresponding Fig. 4.5.

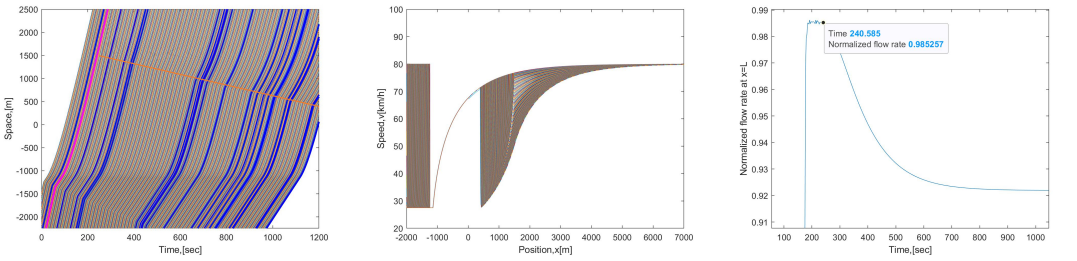

(a) Vehicle trajectories of real vehicles **(b)** Speed profile of real vehicles **(c)** Evolution of queue discharge flow rate at x=L

Figure 4.5: Numerical example for case 2 with 95% MPR. In (a), the blue line shows the trajectories of all NCVs, the pink line represents the trajectory of the first vehicle that encounters a slowdown caused by congestion, and the yellow line shows the shock wave.

In Fig 4.5(a), the blue line represents the trajectory of all NCVs, while the pink line represents the trajectory of the first vehicle that experiences a significant slowdown due to congestion. The moment when this vehicle reaches the end of the bottleneck marks the beginning of the descent in the curve shown in Fig 4.5(c). In this case, the 21^{st} vehicle is the first NCV, while the 27^{th} vehicle is the first vehicle with a significantly reduced speed. Only one blue trajectory lies ahead of the pink trajectory, indicating that congestion immediately occurs at the first NCV, and it rapidly intensifies after propagating backwards. By propagating through six vehicles, a reduction in the normalised traffic flow rate at the end of the bottleneck becomes visible.

When a platoon consists of both CVs and NCVs, only CVs are subject to the speed limit within the VSL zone. As the CV before the first NCV exit the VSL zone and starts acceleration, the NCV following also accelerates, even if it is still within the VSL zone. This results in insufficient spacing between this NCV and the CV ahead of it. Thus, after arriving somewhere within the bottleneck, the speed of this NCV is determined by the congested stationary state instead of the bounded acceleration state. Therefore, the capacity drop can not be prevented (Martínez and Jin, 2020). The congestion intensifies as it propagates upstream, eventually causing an obvious capacity drop phenomenon at the end of the bottleneck.

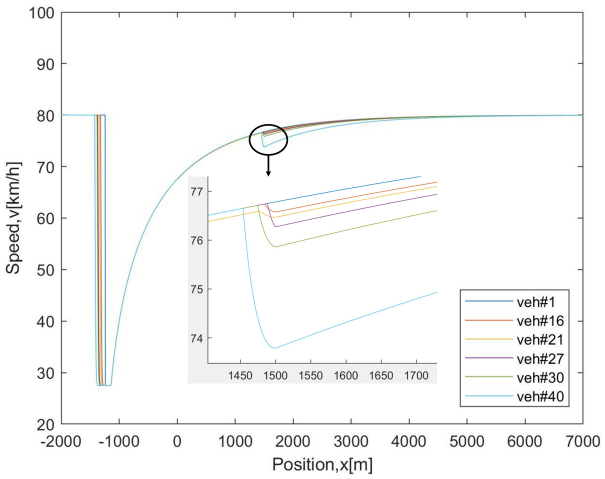

Figure 4.6: Speed profiles of 1^{st},16^{th},21^{th},27^{th},30^{th},40^{th} real vehicle

In Fig 4.6, the speed profiles of vehicles before the 21^{th} vehicle show a smooth increase at the bounded acceleration rate after the VSL zone. The small drops of the 16^{th} can be attributed to numerical errors. However, for vehicles after the 21^{th} vehicle, there is an abrupt decrease in speed within the bottleneck, indicating the transition from the bounded acceleration state to the congested state.

4.5. Scenario 3: the influence of MPR of CVs on the optimal acceleration length

In scenario 2, it has been observed that when the MPR of CVs is below 100%, applying VSL with the parameters determined by Martínez and Jin (2020) does not effectively prevent the capacity drop phenomenon. To further investigate the impact of the acceleration length on capacity drop prevention, scenario 3 is designed. In this scenario, the speed limit of VSL remains the maximum speed limit VSL_{max}, but the acceleration length is no longer fixed. The cases in scenario 3 involve different MPR values of CVs ranging from 100% to 0%. For each case, simulations are conducted with various acceleration lengths to find the minimum feasible acceleration length that effectively prevents the capacity drop phenomenon for that particular MPR value. To prevent impractical acceleration and the potential disruption to the ramp traffic, an upper bound of $2500m$ is set for the acceleration length. This constraint for the maximal allowable acceleration length may vary depending on the prevailing traffic conditions and the characteristics of the road environment. Simulation results are obtained and rounded up, which are summarized in Table 4.5.

Table 4.5: Summary of simulation results for scenario 3

Case	1	2	3	4	5	6	7	9	9
MPR	100%	95%	85%	75%	65%	55%	50%	25%	0% (Base case)
Speed limit (km/h)	27.5								
Required acceleration length from simulations (m)	1140	1260	1370	1500	1700	1920	2485	/	/
Flow rate at the bottleneck (veh/h)	1478.2								
Prevention capacity drop or not	Yes	Yes	Yes	Yes	Yes	Yes	Yes	No	No

The study concludes that increasing the acceleration length is an effective approach to prevent the capacity drop phenomenon when applying the maximum speed limit, particularly for MPR of CVs lower than 100% but greater than 50%. The results indicate that when the speed limits are the same, platoons with lower MPR values of CVs require a longer acceleration length compared to platoons with higher MPR values. This longer acceleration length is necessary to ensure that all vehicles within the bottleneck can accelerate at a bounded acceleration rate. However, it is important to note that increasing the acceleration length may not always be feasible. For MPR values lower than 50%, the feasible acceleration length may either exceed the practical limit of $2500m$ or may not exist at all. Therefore, alternative strategies may be required to effectively prevent the capacity drop phenomenon in such cases.

Various fitting methods are utilized and compared to find the best fit for the simulation results in scenario 3 and to align the curve pattern with the expected trend. Specifically, the exponential function of degree 2 and the polynomial function of degree 4 are considered. They both successfully captured the anticipated trend where the optimal acceleration length decreases as the MPR increases. Also, when evaluating the goodness of fit, both simulation methods exhibit a higher R-squared value. The exponential fitting outperformed the polynomial function as it involves fewer variable degrees. On the other hand, fitting the curve with the sine function resulted in a high R-squared value, but the pattern of variation indicated by the fitted curve could not be confirmed by the data or explained theoretically. As a result, the exponential function of degree 2 is chosen as the preferred fitting method for scenario 3. The fitting curves using different fitting methods are displayed in Fig 4.7.

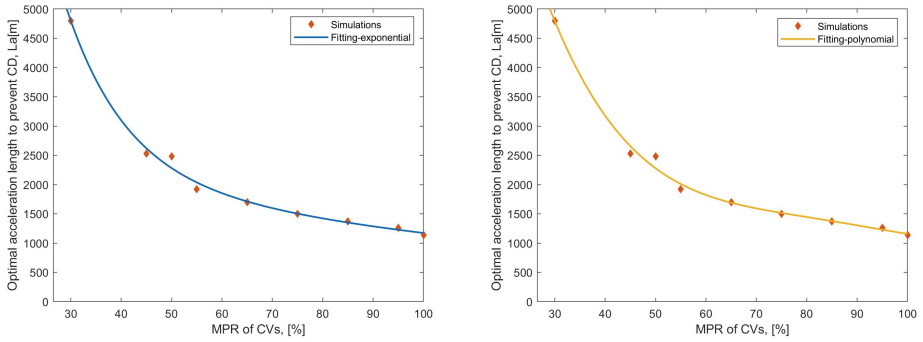

(a) The fitting using exponential function with two degrees

(b) The fitting using the polynomial function with four degrees

Figure 4.7: Comparison of fitting methods for optimal acceleration length for different MPR of CVs with the maximal speed limit

The selected fitting with the exponential function of degree 2 results in a high-quality fit with an R-square value of 0.9937.

4.6. Scenario 4: the influence of MPR of CVs on the speed limit

In this scenario, we assume there is no acceleration zone between the VSL zone and the bottleneck. To achieve the objective of utilizing CVs to enhance the bottleneck throughput, this scenario is designed to identify the maximal speed limit to ensure that the capacity drop can be effectively prevented, without the acceleration zone. Simulations are conducted for cases with different MPR of CVs. The results are listed in Table 4.6.

Table 4.6: Summary of simulation results for scenario 4

Case	1	2	3	4	5	6	7	8	9	10
MPR	100%	95%	85%	75%	65%	50%	35%	25%	20%	0% (Base case)
Maximal speed limit to prevent capacity drop (km/h)	26.74	26.71	26.68	26.65	26.62	26.59	26.51	25.70	24.83	/
Flow rate at the bottleneck (veh/h)	1478.2	1463.3	1459.5	1460.4	1459.8	1458.4	1457.6	1448.7	1419.8	1380.6
Prevention capacity drop or not	Yes	Yes	Yes	Yes	Yes	Yes	Yes	Yes	Yes	No

The analysis reveals that when the acceleration length is set to $0m$, there is no significant difference in the maximal speed limit to prevent capacity drop for cases with MPR of CVs above 50%. This implies that without the acceleration zone, the potential advantages of a high MPR of CVs cannot be fully realized. However, when the MPR of CVs falls below 50%, the maximum speed limit to prevent capacity drop decreases as the MPR decreases. At 20% MPR of CVs, the maximum feasible speed limit approaches the lower bound of the speed limit range.
The fitting for simulation results in scenario 4 is shown in Fig.4.8. The determination of the fitting method is the same as the method described in section 5.3.1.

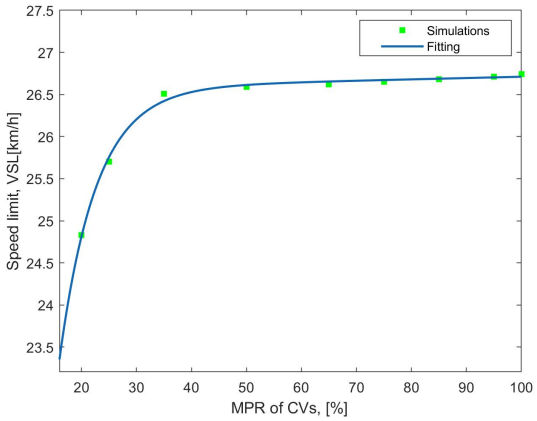

Figure 4.8: Exponential fitting: maximal speed limit to prevent capacity drop for different MPR of CVs without acceleration length

Fig. 4.8 is fitted using an exponential function with two degrees. The R-square value of 0.9958.

4.7. Scenario 5: the relationship among the speed limit, the acceleration length and MPR of CVs

The simulation results from scenarios 3 and 4 highlight that adjusting the speed limit or acceleration length independently is not sufficient to prevent the capacity drop when considering different MPR values for CVs. When the MPR falls below 50%, solely increasing the acceleration length does not enable VSL with the maximum speed limit (VSL_{max}) to effectively prevent the capacity drop. Similarly, changing the speed limit alone does not fully capitalize on the advantages of a high MPR for CVs.

To address these limitations, several values of speed limits within the predetermined range are tested for cases with MPR values of 100%, 75%, 50%, and 25%, respectively. Based on the conclusions drawn from scenario 3 regarding the maximal speed limit capable of preventing the capacity drop with an acceleration length of $0m$, multiple points within the range between this value and the maximum speed limit (VSL_{max}) are selected as tested speed limits for each case in the simulations. By analyzing the simulation results, the optimal acceleration length required to prevent the capacity drop for each case with a specific speed limit and MRP of CVs is determined. The simulation results are listed in Table A.1 in appendix a and reveal important findings regarding the relationship between the MPR of CVs, the applied speed limit, and the required acceleration length to prevent capacity drop.

The analysis confirms two key findings. Firstly, for a given MPR of CVs, the optimal acceleration length remains as $0m$, then increases exponentially as the speed limit increases. This suggests the rules proposed by Martínez and Jin (2020) that for speed limits higher than certain values, the higher speed limits necessitate longer acceleration lengths to prevent capacity drop still holds when the MPR of CVs is not 100%. Meanwhile, when comparing different speed limits for the same MPR of CVs, it is found that the required additional length of acceleration, compared to the length needed for the case with 100% MPR, also increases as the speed limit increases. Secondly, when the VSL adopts a relatively lower speed limit, the simulation results show that an acceleration length of $0m$ is sufficient to prevent capacity drop across all analyzed levels of MPR of CVs. However, when the VSL adopts a higher speed limit, cases with lower MPR of CVs require longer acceleration lengths to prevent capacity drop. The goal of having the highest possible speed limit is to have the highest flow. But the findings suggest that the MPR of CVs influences the acceleration length when the VSL employs a high-speed limit. It is not always feasible to adopt as high a speed limit as possible when implementing VSL in practical situations. Instead, an ideal approach to VSL implementation involves striking a balance between speed limits and acceleration lengths. A relatively smaller speed limit can achieve several advantages, while not significantly reducing flow. Firstly, the obstruction of ramp traffic due to long acceleration distances can be mitigated. Additionally, utilizing a smaller speed limit helps avoid the influence of varying levels of MPR of CVs (or driver compliance) on the control effect of the VSL system, which ensures consistent and reliable performance of the VSL.

When the MPR of CVs is 25%, the required optimal acceleration length to prevent capacity drop un-

der the same speed limit is increased compared to the higher MPR of CVs. What's more, there is a significant level of uncertainty in the simulation results. Despite keeping all simulation parameters unchanged, the occurrence of the capacity drop may vary across different runs of the same scenario. The capacity drop may be prevented in some runs, while in others, it may occur. This highlights the inherent uncertainty associated with lower MPR of CVs and emphasizes the challenges in implementing practical control strategies under such conditions. The results presented in Fig. 4.9 prevents capacity drop for the 5 runs with MPR 25%. When the MPR of CVs is less than 25% and the speed limit is relatively high (higher than $27km/h$), the prevention of capacity drop requires an extremely long acceleration length which is unrealistic. Thus, it's concluded that the capacity drop can not be prevented in these cases.
The fitting for simulation results in scenario 5 is presented in Fig.4.9.

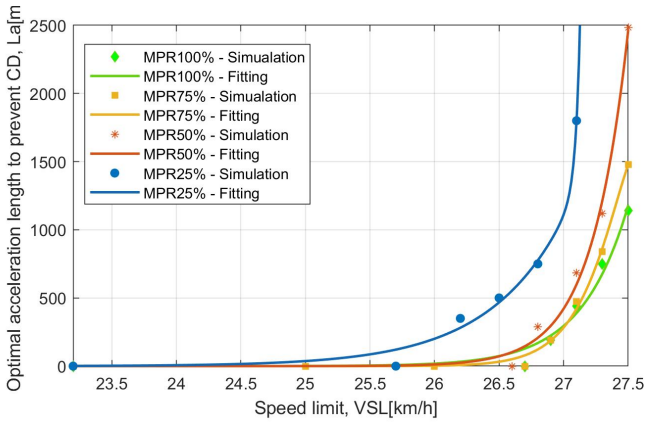

Figure 4.9: Exponential fitting: the relationship between the speed limit and optimal acceleration length for various MPR of CVs

The fitting using the exponential method with two degrees yields good results. The R-square values for fitting 100%, 75%, 50%, and 25% MPR of CVs are 0.9739, 0.9952, 0.9924, and 0.9906, respectively.

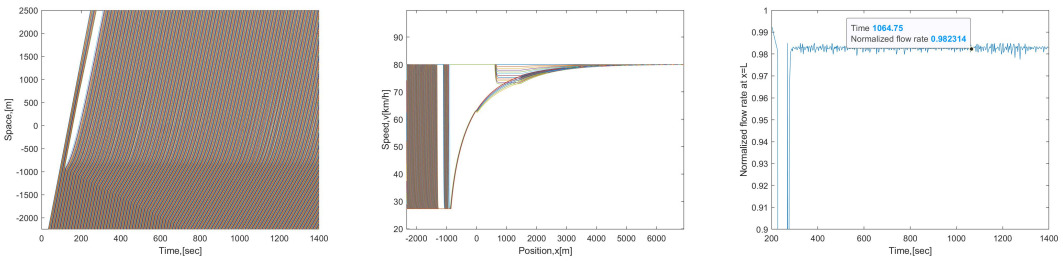

(a) Vehicle trajectories of real vehicles **(b)** Speed profile of real vehicles **(c)** Normalized traffic flow rate at x=L

Figure 4.10: Numerical example for the case with 75% MPR of CVs, and employing VSL with a speed limit of $27.3km/h$ and an acceleration length of $850m$

With the case of 75% MPR of CVs, the impact on the travel time of a different VSL setting, compared to the one in section 4.4.1, is analyzed. This different VSL strategy involves a speed limit of $27.3km/h$ and an acceleration length of $850m$. The simulation results are shown in Fig 4.10. The travel time for selected vehicles and the average travel time are calculated based on the simulation results are listed in Table 4.7

Table 4.7: Travel time comparison for the new VSL

Vehicle number	Arrive time at the bottleneck end $T(n)$	Travel time, (s)			Improvement	
		Without VSL		VSL		
		Low demand	High demand	High demand	Difference	Percentage (compare to the travel time in base case 2)
100^{th}	Within the transition period	360	419.5	434.8	-15.3	-3.6%
200^{th}			470.6	470.2	-0.4	-0.1%
250^{th}			495.8	488.4	7.4	1.5%
300^{th}	After the transition period		521.0	505.8	15.2	3%
400^{th}			586.0	541.2	44.8	7.6%
Average of all 450 vehicles	/		483.4	469.4	14.0	2.9%

In this case, congestion initially occurs, but it is later resolved by the VSL strategy, which creates gaps between vehicles. The capacity drop phenomenon is effectively prevented through this VSL approach. Additionally, the travel time of individual vehicles located after the 250^{th} position is reduced compared to the uncontrolled scenario when the demand is high. Moreover, the average travel time of all 450 simulated vehicles demonstrates considerable improvement compared to the uncontrolled scenario with high demand. The impact of this VSL strategy on travel time is more pronounced than the one observed in the previous VSL scenario discussed in section 4.4.1.

5

Sensitivity analysis

In this chapter, the sensitivity analysis of simulation results is performed to investigate the impact of different factors on the effectiveness of VSL control. To analyze the influence of the bottleneck length on the capacity drop and the relationship between VSL parameters and MPR of CVs, a $500m$ tunnel bottleneck is simulated and compared to the results from the $1500m$ bottleneck in section 5.1. In section 5.2, the impact of bounded acceleration assumptions on the minimal MPR to validate the work of Martínez and Jin (2020) is analyzed. A Constant Bounded acceleration (CBA) model which produces capacity drop similar to the TWOPAS model is adopted. The minimal required MPR to enable the highest speed limit and the acceleration length calculated by Martínez and Jin (2020) is investigated with the CBA model. In section 5.3, the influence of random CV positions within the platoon on the time when the flow starts to drop is shown. In section 5.4, the impact of the transmission delay which leads to the delayed activation of VSL on the prevention of capacity drop is studied.

5.1. The influence of the bottleneck length on the capacity drop and VSL strategies

Based on the calibrated data from the Kobotoke tunnel in Japan, the speed limit range obtained by Eq.3.8 and Eq.3.9 results in a very narrow range. In practical terms, such a small variation in speed limits may not be easily perceptible by drivers. To ensure the practicality of the conclusions regarding the influence of the MPR of CVs on the interplay between the speed limit and acceleration length, a similar tunnel bottleneck with a shorter length is studied. Specifically, some of the parameters in Table 4.1 are adjusted, where the bottleneck length is reduced from $1500m$ to $500m$. The value of the time gap at the entrance of the bottleneck is maintained at $1.5s$, while the time gap at the bottleneck end is modified to $1.7s$ to maintain the same ratio of $(\tau_2 - \tau_1)/L$. Additionally, the high demand is adjusted to be slightly higher than the resulting new bottleneck capacity after the adjustment. All other inputs into the simulation remain unchanged. The values of the adjusted parameters are listed in Table 5.1 below. The symbol * indicates that the value of the variable has changed. The base case 2 in scenario 1, scenario 2 and scenario 5 described in Table 3.1 are simulated with these adjusted parameters.

Table 5.1: Adjusted parameters of the simulation

Parameter	Value	Unit
Free-flow speed, v_f	80	km/h
Jam density, k_j	140	veh/km
Maximum acceleration rate on a level road, a_0	0.407	veh/s^2
Decimal grade at x, $\phi(x)$	0	—
Bottleneck length, L^*	0.5	km
Time gap upstream to the bottleneck, τ_1	1.5	s
Highest time gap inside the bottleneck, τ_2^*	1.7	s
Capacity of the start of tunnel, C_1	2000	veh/h
Capacity of the end of tunnel, C_2^*	1781	veh/h
High Demand, D_2^*	1870	veh/h
The number of simulated real vehicles, n_v	450	veh
The simulated time, t_f	1200	s
The length of VSL zone, L_{VSL}	100	m

5.1.1. The minimal MPR of CVs to achieve the highest flow

The simulation results for the base case 2 are shown in Fig. 5.1. The capacity drop can be still observed in this case which its characteristics, namely the duration of the transition period and the dropped stationary capacity, differ. In the case of the longer bottleneck ($1500m$), the transition period is $16mins$ and the dropped capacity is $1380veh/km$. In the case of the shorter bottleneck, the transition period is $14mins$ and the dropped capacity C_3^* is $1632veh/km$. The ratio of dropped capacity is 8.4%, which is within the empirical range from 3% to 18% (Oh and Yeo, 2012). Based on the results, the wider range of speed limit of VSL is calculated using the method described in section 3.2.1, which is from $36.5km/h$ to $49.0km/h$. To avoid obtaining infinite acceleration length (explained in section 4.1, the maximal speed limit is slightly rounded down to $48.5km/h$.

The VSL used for scenario 2 employs a speed limit of $48.5km/h$. Since the optimal acceleration length calculated using Eq. 3.11 is $3060m$, the upper constraint of the acceleration length is extended to $5000m$. Simulation results confirm that capacity drop can be prevented with this VSL when the MPR of CVs is 100%. However, when the VSL strategy is applied with an MPR of 95% of CVs, capacity drop occurs, see Fig. 5.2. This suggests that the MPR needed to achieve effective control with the VSL strategy proposed by Martínez and Jin (2020) is not influenced by the bottleneck length and remains at 100%.

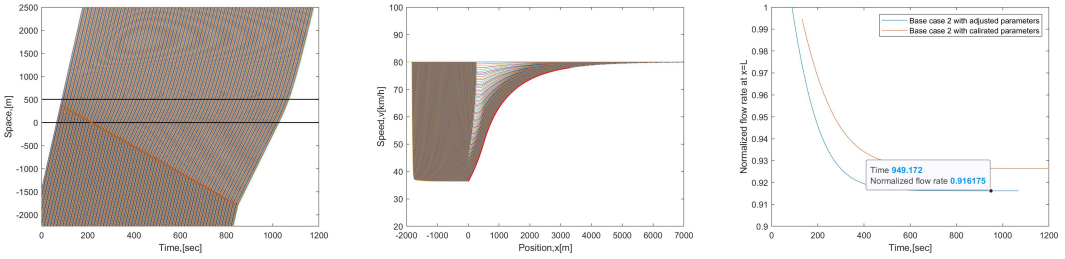

(a) Vehicle trajectories of real vehicles **(b)** Speed profile of real vehicles **(c)** Evolution of queue discharge flow rate at x=L

Figure 5.1: Numerical example with adjusted parameters for scenario 1 case 2

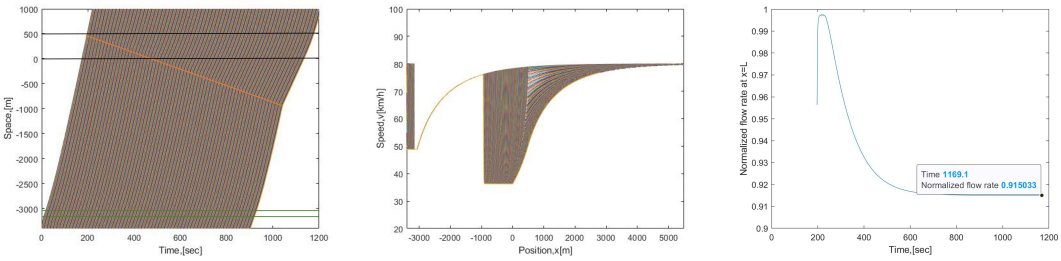

(a) Vehicle trajectories of real vehicles **(b)** Speed profile of real vehicles **(c)** Evolution of traffic flow rate at x=L

Figure 5.2: Numerical example for scenario 2 case 2 with adjusted parameters

5.1.2. The relationship between speed limit, acceleration length and MPR of CVs

Here, the cases with 100%, 75%, 50%, 25% MPR of CVs are simulated. For each case, several speed limits within the range are predetermined as inputs into the VSL control, and the corresponding optimal acceleration lengths are identified in simulations. The simulation results are listed in Table A.2.

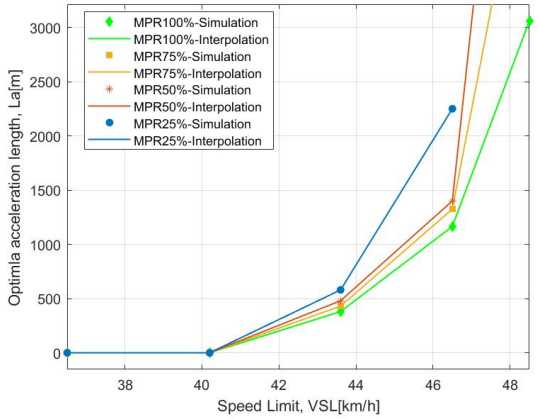

Figure 5.3: Interpolation: the relationship between the speed limit and optimal acceleration length for various MPR of CVs with $500m$ bottleneck length

The relationship between the MPR of CVs and the VSL parameters for the $500m$ tunnel bottleneck exhibits a similar trend to the results obtained for the $1500m$ bottleneck. For a given MPR, as the speed limit increases from the minimum to the maximum, the initial acceleration distance stays at $0m$ and then gradually increases. Smaller MPR of CVs leads to a more obvious subsequent increase. If the applied speed limit is below a critical value, which depends on bottleneck conditions, the required acceleration distance is always $0m$ regardless of different MPR of CVs, which means the acceleration zone is not required between the end of the VSL zone and the bottleneck. However, when the speed limit is higher than the critical value, a smaller MPR of CVs results in a longer required acceleration distance before entering the bottleneck, compared to scenarios with higher MPR levels of CVs. Notably, when the MPR is 50% and the maximum speed limit is used, even with an acceleration length of $8000m$, the VSL fails to prevent capacity drop. This finding reinforces the findings in section 4.7 which suggest that achieving a balance among the speed limit, the required acceleration length, and the reliability of VSL effectiveness across different levels of MPR of CVs is crucial in VSL applications.

5.2. The influence of bounded acceleration assumptions

One of the essential assumptions in this study is the utilization of the TWOPAS model of the bounded acceleration, as described in Eq. 3.4. This model plays a critical role in shaping the acceleration patterns of vehicles by imposing an upper limit on their acceleration. In situations where capacity drop occurs, the acceleration rate of vehicles after passing downstream of the bottleneck is determined by this model. When the VSL is implemented and capacity drop is successfully prevented, vehicle

acceleration adheres to the TWOPAS model in both the acceleration zone and the bottleneck area before reaching the free-flow speed.
To assess the influence of bounded acceleration assumptions on traffic dynamics, the CBA model (see E.q. 5.1) is considered in this section. The CBA model is employed in two specific scenarios: base case 2 in scenario 1 and scenario 2. In base case 2 of scenario 1, the aim is to evaluate the impact of different acceleration assumptions on the capacity drop and its characteristics. Scenario 2 focuses on evaluating the effect of different bounded acceleration assumptions on the minimum MPR of CVs required to validate the conclusions and formulas derived from the work of Martínez and Jin (2020). In both scenarios, all other parameters are kept consistent with the parameters used in simulations conducted with the TWOPAS model. By comparing the results obtained from the CBA model to those obtained from the TWOPAS model, the study allows for a comprehensive understanding of how the bounded acceleration model influences the outcomes of the study and gains insights into the robustness and reliability of its findings. The CBA model adopted for the comparative analysis can be expressed using the equation:

$$A_{max}(x, v) = a_{con} \tag{5.1}$$

where a_{con} is a constant. In the simulation, various values of a_{con} are tested to determine their influence on the queue discharge rate at the end of the bottleneck. And $(3/8) * a_0$ is identified to produce a curve most similar to the one obtained when simulating with the TWOPAS model. This ensures a meaningful comparison between the results obtained from the CBA model and the TWOPAS model.
The speed profiles for all real vehicles in the base case 2 with the CBA model of $(3/8) * a_0$ are shown and compared to the speed profiles when using the TWOPAS model, see Fig. 5.4.

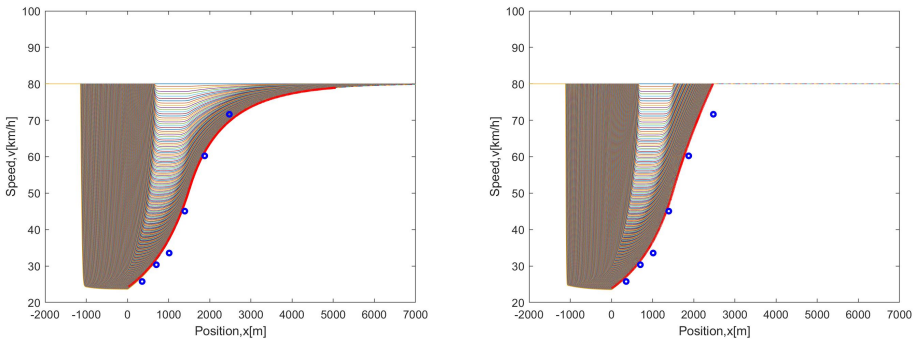

(a) Speed profiles with TWOPAS model

(b) Speed profiles with CBA model $((3/8) * a_0)$

Figure 5.4: Speed profiles with different bounded acceleration models and Koshi et al. (1992) data

It can be seen that the two bounded acceleration models eventually lead to different converging acceleration curves for vehicles driving out of the queue. The converged speed profile from the TWOPAS model is more consistent with empirical data from Koshi et al. (1992). The evolution of the queue discharge rate at the end of the bottleneck with different bounded acceleration models is presented in Fig. 5.5.

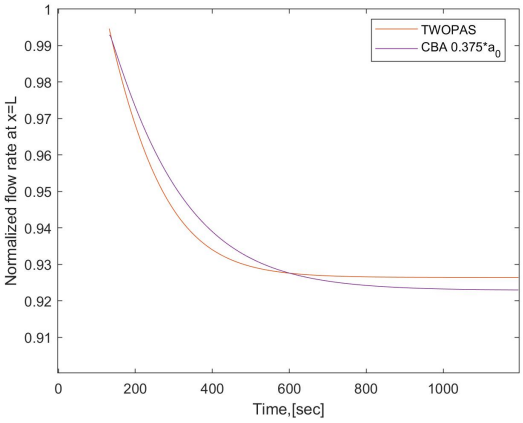

Figure 5.5: Comparison of queue discharge rate with different bounded acceleration assumptions

Despite employing distinct acceleration assumptions, the TWOPAS model and the CBA model with a value of $(3/8) * a_0$, lead to a similar capacity drop phenomenon. The evolution of the queue discharge rate at the bottleneck neck and the flow at the capacity drop stationary state is not significantly different between the two models. Based on the findings presented in section 5.2, it is concluded that the minimum MPR of CVs required to prevent capacity drop is found to be 100% when implementing VSL with the speed limit and acceleration length calculated by Eq. 3.11. Simulations for scenario 2 are repeated with the CBA assumption. The results are listed in Table 5.2.

Table 5.2: The minimum MPR of CVs to prevent capacity drop

Bounded acceleration model	Speed limit (km/h)	Acceleration length calculated by Eq. 3.11(m)	the minimum MPR (%)
TWOPAS	27.5	1140	100%
CBA((3/8)*a_0)		0	40%

The utilization of the CBA model yields a minimum MPR value of 40% for effective VSL control, which differs significantly from the 100% determined by the TWOPAS model. This discrepancy highlights the substantial impact of bounded acceleration on the VSL control effectiveness. It emphasizes the importance of selecting and calibrating the appropriate bounded acceleration model when modelling vehicle dynamics and implementing VSL strategies.

5.3. The influence of different positions of CVs on capacity drop

For a given MPR, CVs maintain the fixed proportion of all vehicles, while their positions within the platoon are randomly assigned. To illustrate the impact of the arrangement of CVs within a platoon on the timing of the flow starts to drop, we consider a scenario with a 50% MPR of CVs. This particular MPR ensures noticeable variations in the order of CVs among different simulation runs. We apply VSL control with a speed limit of $27.3km/h$ and an acceleration length of $1000m$. In section 5.5, it is concluded that when applying a speed limit of $27.3km/h$ to a 50% MPR of CVs, a minimum acceleration length of $1120m$ is required to effectively prevent capacity drop. Consequently, with an acceleration length of only $1000m$, it is expected that capacity drop cannot be prevented.
We conduct three simulation runs of this case, each run generating different orders of CVs within the platoon. The simulation results exhibit varying timings of the flow starting to drop, as depicted in Fig. 5.6.

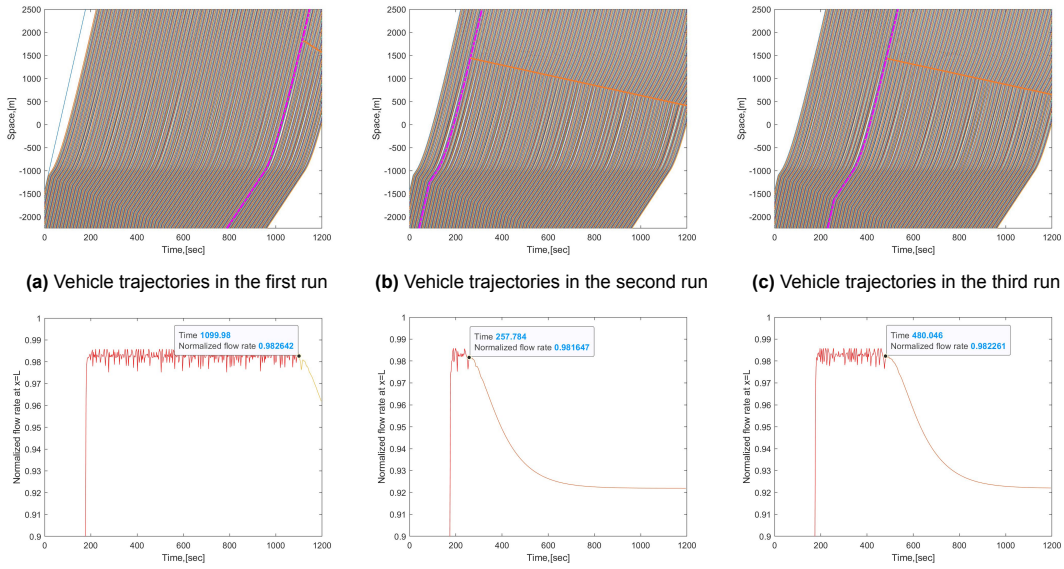

(a) Vehicle trajectories in the first run **(b)** Vehicle trajectories in the second run **(c)** Vehicle trajectories in the third run

(d) Evolution of queue discharge flow rate in the first run **(e)** Evolution of queue discharge flow rate in the second run **(f)** Evolution of queue discharge flow rate in the third run

Figure 5.6: The timing of capacity drop caused by different orders of CVs

From the analysis of Fig. 5.6(d)(e)(f), we can identify the approximate time point when the flow starts to drop. At this moment, we consider the vehicle located at the end of the bottleneck as the first vehicle to encounter congestion within the bottleneck. The trajectory of this vehicle is indicated by the pink dashed lines in Fig. 5.6(a)(b)(c). Upstream of this vehicle, the traffic flow remains stable at a high level, equal to the outflow of the VSL zone. However, after this specific vehicle, congestion propagates upstream along the yellow lines and the queue discharge rate begins to decrease.
The position of this first vehicle experiencing a sudden change within the bottleneck varies across the three simulation runs. In the first run, it appears as the 380^{th} vehicle, while in the second run, it emerges as the 38^{th} vehicle. In the third run, it is positioned as the 128^{th} vehicle. This variability highlights the significant influence of the randomness in the arrangement of CVs on the timing of the flow starts to drop.

5.4. The influence of transmission delay on VSL effectiveness

In the previous simulations, VSL is assumed to be activated and implemented immediately when inputting the high demand. However, in reality, practical constraints within the operational procedures of the control system introduce a certain delay before the VSL can be fully functional. This delay could be due to various factors such as signal processing, communication delays, or coordination between controllers and infrastructures.
To understand the influence of this transmission delay on the effectiveness of VSL control, the comparative analysis compares two cases: immediate VSL implementation and a $2mins$ delay before VSL implementation. Both cases are tested with 100% MPR of CVs and 75% MPR of CVs. The input constant demand is D_2. The VSL parameters used for this analysis include a maximal speed limit of $27.5km/h$, an optimal acceleration length of $1140m$ when the MPR of CVs is 100% and an optimal acceleration length of $1500m$ when the MPR of CVs is 75%. In section 4.7, it's validated through simulations that the capacity drop can be prevented if the VSL is applied to all CVs immediately after the detection of the high demand. The results from simulations with $2mins$ delay of VSL application are shown in Fig. 5.7.

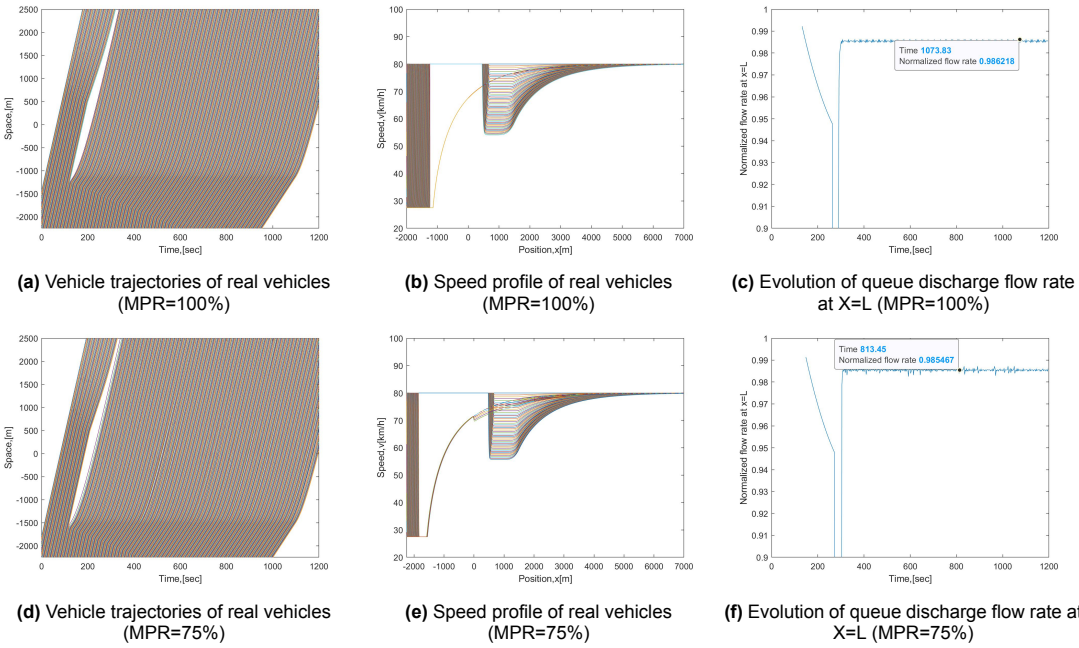

(a) Vehicle trajectories of real vehicles (MPR=100%)

(b) Speed profile of real vehicles (MPR=100%)

(c) Evolution of queue discharge flow rate at X=L (MPR=100%)

(d) Vehicle trajectories of real vehicles (MPR=75%)

(e) Speed profile of real vehicles (MPR=75%)

(f) Evolution of queue discharge flow rate at X=L (MPR=75%)

Figure 5.7: Numerical example for the case with transmission delay

The comparative analysis reveals that even with a transmission delay of $2mins$ before VSL implementation, the capacity drop can still be effectively prevented with both 100% MPR of CVs and 75% MPR of CVs. Despite the initial congestion built up by the high inflow before VSL activation, the reduced speed of the CVs after VSL implementation creates a gap, allowing for congestion dissipation. This finding suggests the robustness and effectiveness of VSL control strategies in real-world scenarios where transmission delays are present.

6

Conclusions

This research explores the impact of VSL control in a mixed traffic environment. The study provides supplementary findings to previous work, emphasizes the importance of considering MPR when determining speed limits and acceleration lengths, and suggests the further analysis of different bottleneck models. Practical limitations in the open-loop VSL approach in this thesis exist, such as real-time traffic measurements and speed deceleration assumptions. Future studies are encouraged to analyze the influence of MPR of CVs in multi-lane traffic, considering traffic heterogeneity, and establish a closed-loop VSL control system that enables the automated adjustment of control signals to solve congestion.

6.1. Answer to research questions

The results obtained from this study address the main research question and its associated sub-questions as follows:

Sub question 1:
What is the current state-of-the-art of using CVs in VSL to prevent capacity drop? Are there any limitations or challenges that need to be addressed before this technology can be fully implemented?
Answer: The utilization of CVs in VSL strategies to prevent capacity drop is an emerging field of research. Relying on equipped sensors, CVs serve as detectors for gathering real-time traffic data with higher precision and flexibility compared to fixed-location loop detectors. By sharing data with other vehicles and roadside infrastructures, CVs enable dynamic information transmission. CVs can also receive personalized driving instructions from controllers via telecommunication technologies, functioning as actuators. This allows for the development of proactive traffic management to enhance the efficiency of transportation networks.
Researchers explore different approaches to implementing VSL in CV environments, aiming to optimize traffic control and improve overall performance (Lee and Park, 2013; Han et al., 2017). It has demonstrated that the MPR of CVs plays a significant role in determining the effectiveness of VSL strategies. This highlights the need for careful consideration of the MPR of CVs when designing and implementing VSL in CV environments, including the determination of control laws and control parameters. It is important to note that the deployment of CVs in real-world traffic management is still in its design stages. Before the implementation in the real world, a threshold MPR of CVs is expected to realize.

Sub question 2:
Which existing models are best suited to modelling vehicle behaviour and capacity drop in sag and tunnel bottlenecks for this study? What assumptions and simplifications are necessary, and how can we validate its predictions against real-world data?
Answer: There are multiple models that can be used to reproduce capacity drop. The research utilizes the continuum car-following model proposed byWada et al. (2020) which assumes an inhomogeneous triangular fundamental diagram and bounded acceleration rate. This model discretizes real vehicles into imaginary vehicles, forming a continuum traffic flow and updating the driving behaviour of imaginary

vehicles at each time step. To simplify the analysis, it focuses solely on longitudinal driving behaviour and captures the effect of a reduced capacity with an increasing time gap linearly.
This model effectively captures the observed capacity drop at the end of the bottleneck and facilitates a clear understanding of the relationship between microscopic behavioural rules and macroscopic phenomena. The model includes limited number of parameters to be calibrated and validated. The variables of this model possess physical interpretations, enabling straightforward investigations into the physical and mathematical properties of the traffic system. Moreover, the model is specifically designed to reproduce the capacity drop stationary state which is stable and less complex. It successfully reproduces the transition period from the onset of congestion to the converged queue discharge rate.

Sub question 3:
What are key parameters in the VSL approach that need to be considered when implementing a CV-based open-loop VSL control strategy, and how do these parameters interact?
Answer: The speed limit and acceleration length are critical parameters in the implementation of VSL, as they directly impact the controlled traffic flow and the prevention of capacity drop. The speed limit applied in VSL regulates the inflow into the bottleneck. The maximal speed limit should lead to a flow lower than the bottleneck capacity, while the minimum speed limit should result in a flow higher than the capacity after the congestion. On the other hand, Martínez and Jin (2020) highlights the significance of the acceleration length in preventing capacity drop. The acceleration length refers to the distance between the end of the VSL zone and the entrance of the bottleneck, within which vehicles need to accelerate to reach the desired speeds.
The relationship between the speed limit and the required acceleration length is noteworthy. As Martínez and Jin (2020) discover, a higher speed limit necessitates a longer acceleration length. This acceleration length must enable vehicles to surpass the speed limit at the bottleneck entrance and ensure that the speed at the end of the bottleneck exceeds the speed determined by the congested branch of the downstream fundamental diagram associated with the controlled flow.

Sub question 4:
What is the minimum MPR of CVs to enable an open-loop VSL to achieve the maximal flow in the study's context? What variables impact this minimum MPR value?
Answer: This study focuses on applying VSL to CVs, and it is assumed that all CVs comply with the VSL control. By investigating the minimum MPR necessary to prevent capacity drop, the study also establishes the precondition for the conclusions of Martínez and Jin (2020) to be valid in terms of driver compliance with the control.
Specifically, it is demonstrated that when the TWOPAS model is assumed, the MPR of CVs must be 100% for the conclusions of Martínez and Jin (2020) to hold. Additionally, the study finds that this minimum MPR is influenced by the assumptions of the bounded acceleration model used.

Sub question 5:
How can the VSL parameters be adjusted considering different MPR of CVs to prevent capacity drop at sag and tunnel bottlenecks?
Answer: In the simulation, certain parameters are held constant while employing the dichotomy method to adjust the value of the analyzed parameters in each scenario based on simulation results. Specifically, the MPR of CVs and the speed limit are fixed, and the minimum acceleration length required to prevent capacity drop is determined using the dichotomy method based on the value of acceleration length obtained through formulas proposed by Martínez and Jin (2020). Similarly, when the MPR is fixed and the acceleration length is set to $0m$, the dichotomy method is employed to narrow down the range of feasible speed limits that can prevent capacity drop. This process continues until the maximum speed limit to prevent capacity drop in each case is identified.

Sub question 6:
What is the impact of assumptions made in modelling and simulations on research results?
Answer: In this thesis, several variables are considered and analyzed to understand their impact on the simulation results. The variables include the bottleneck length, the assumption of bounded acceleration, and the transmission delay in the VSL implementation. To assess the influence of bottleneck length, simulations are conducted using a tunnel bottleneck with a length of 500m, and the results are

compared to simulations with a tunnel bottleneck of $1500m$ in length. This analysis provides insights into how the length of the bottleneck affects the capacity drop phenomenon and the relationship between the MPR of CVs and the VSL parameters. The CBA model is used to reproduce the similar capacity drop phenomenon observed in the TWOPAS model. The threshold MPR of CVs that ensures the conclusions by Martinez et al. hold, obtained from the CBA model is compared to the 100% MPR derived from the TWOPAS model. Another variable considered is the transmission delay of the VSL system. Simulations are performed with immediate activation of VSL and with a $2minus$ delay in the transmission of control signals. By comparing the simulation results, the influence of transmission delay on the effectiveness of VSL control is assessed.
During the simulation, vehicles and time are discretized. Numerical errors are introduced, and convergence analysis is conducted to determine the largest discrete unit that ensures convergence of the simulation results. And to mitigate the influence of the randomness in the positions of CVs within the platoon on the experimental results, multiple repetitive experiments are performed for each case, and the conclusions are only drawn when the simulation results from all simulation runs are consistent.

Main question:
How does the MPR of CVs affect the determination of parameter values for CVs-based VSL to ensure effectiveness in preventing capacity drop at sag and tunnel bottlenecks?
Answer: The finding is based on simulation results utilising the continuum car-following model with the TWOBAS bounded acceleration model and applied on the tunnel bottleneck which is assumed a linear increasing time gap within the bottleneck (Wada et al., 2020) .
For a certain MPR of CVs, there is a critical threshold value for the speed limit, beyond which the required acceleration length increases exponentially. This threshold depends on the bottleneck geometry and traffic conditions. For example, when the MPR of CVs is 75%, the threshold of the speed limit is $26.7km/h$ for the simulated $1500m$ tunnel bottleneck in this work. For all speed limits below this threshold, the required acceleration length between the end of the VSL zone and the entrance of the bottleneck to prevent capacity drop is $0m$. This threshold value varies across different MPR of CVs. Regarding the impact of MPR on the required acceleration length for a certain speed limit, the study suggests that as the MPR increases, the required acceleration distance to prevent capacity drop decreases. Additionally, when the acceleration length is fixed and non-zero, a larger MPR of CVs enables to employ of a higher speed limit of VSL while still preventing capacity drop.

6.2. Conclusions and reflections

In summary, this research is conducted based on reproducing the capacity drop phenomenon in sag and tunnel bottlenecks using a continuum car-following model proposed by Wada et al. (2020). It considers a mixed traffic environment with both CVs and NCVs and applies an open-loop VSL control to all CVs. To realize the prevention of capacity drop, the study focuses on quantifying the relationship between the MPR of CVs and the VSL parameters, which are the speed limit and acceleration length in this research.
The research provides supplementary findings to the work of Martínez and Jin (2020) about the optimal application location of VSL for different speed limits. It reveals that a minimum MPR of CVs is necessary for the conclusions of Martínez and Jin (2020) to hold, challenging the thought that controlling only the leading vehicle is sufficient to control the behaviour of all following vehicles. Furthermore, the study demonstrates that this minimum MPR threshold varies depending on the acceleration behaviour of the vehicles. Moreover, the research highlights the significance of considering the MPR of CVs when determining the speed limit and acceleration length of the VSL. It shows that while a higher speed limit can lead to higher throughput, the optimal acceleration length increases exponentially with the increasing speed limit, particularly in cases with low MPR of CVs. While adopting a relatively lower speed limit, the acceleration length can be reduced to $0m$ for all levels of MPR of CVs. It suggests that when implementing VSL in practice, a balance between the resulted throughput, the required acceleration length and the robustness of VSL across different levels of MPR of CVs should be considered.
In this study, the calibrated parameters of the models are based on data from the Kobotoke tunnel in Japan, resulting in a capacity drop ratio of approximately 8%. However, the analysis showed that the feasible range of VSL speed limits calculated by traffic dynamics and road geometry of this tunnel bottleneck is very narrow, with only a small difference of $4km/h$ between the maximum and minimum

speed limits. This small change in speed may be imperceptible to drivers in practice. Additionally, the study found that even a minor reduction in the speed limit significantly reduces the required acceleration length. Thus, it appears that there seems no necessity to adjust the speed limit in VSL based on the findings of this research. Thus, the example bottleneck in Kobotoke is not the best setup to analyse this impact. To address this limitation, it would be beneficial to analyze other bottleneck models that may result in a broader feasible range of VSL speed limits, as a similar analysis was done for the other (hypothetical) bottleneck with a shorter bottleneck length in Section 5.1. Thus, it may be possible to identify scenarios where adjustments to the speed limit can effectively optimize throughput while still ensuring the desired acceleration length and the robustness of VSL across different MPR levels of CVs. Such analysis would provide more practical insights into the implementation of VSL.
Some assumptions made in this research have practical limitations. For instance, the assumption of real-time traffic flow measurements at the end of the bottleneck to visualise the capacity drop phenomenon may not be feasible. The traffic monitoring devices commonly used in the real world are loop detectors. These devices typically provide average traffic flow values over a certain time interval, typically around $30s$. Additionally, the assumption of instantaneous speed reduction to the speed limit simplifies the actual behaviour of vehicles. In reality, vehicles require a certain deceleration time to adjust their speed. This means that the length of the VSL zone needs to be designed to allow sufficient distance for vehicles to gradually decelerate and reach the desired flow and desired speed when they exit the VSL zone.
To manage the computational load, a practical approach is to use the maximal discretize units that ensure convergence of the results in simulations. However, numerical errors can still occur, indicated by deviations from the ideal stationary acceleration pattern of vehicles after the VSL zone when capacity drop can be prevented in the simulation. To enhance the accuracy of the experiments, the simulation algorithms can be streamlined and optimized or a more powerful computer can be utilized.
Another important and complex aspect of the integration of CVs into the traditional traffic control system is the legal issues. Speed limits are legal measures applied to ensure safety and regulate traffic flow. Traditionally, speed limits apply uniformly to all vehicles on a given road section. Applying dynamic speed limits exclusively to CVs may seem unfair to some drivers, potentially leading to division between CV and non-CV drivers and resistance to the technology. While some CV drivers appreciate the safety and efficiency benefits, others value the freedom to drive at their desired speeds. To address these challenges, a comprehensive approach involving policymakers, engineers, manufacturers, and the public is crucial. Some potential solutions could include establishing uniform standards, ensuring effective communication, raising public awareness, and applying enforcement mechanisms.

6.3. Future studies

The literature reveals that traditional VSL methods effectively improve traffic conditions by reducing speed differences and synchronizing driver behaviour. Researchers have explored various control methodologies, including feed-forward and feedback control, to optimize VSL performance. Additionally, the integration of CVs in VSL opens up new possibilities for improving traffic efficiency through timely communication between vehicles and infrastructures. The literature underscores the significance of driver compliance with VSL control signals and how the MPR of CVs influences control effectiveness. Studies consistently demonstrate that higher levels of CVs compliance, or a higher MPR of CVs, lead to increased safety benefits and more substantial travel time savings. This thesis focuses specifically on the impact of VSL control on the capacity drop phenomenon in a mixed traffic environment with CVs. It's discovered that the MPR of CVs plays an important role in determining the effectiveness of VSL strategies in preventing capacity drop at bottlenecks. It became evident that careful consideration of the MPR of CVs is crucial when determining the appropriate speed limits and acceleration lengths for VSL control. However, the real-world implementation of CV-based strategies presents challenges that must be addressed for successful deployment. This thesis can jointly support VSL as a promising approach to prevent capacity drop and enhance traffic flow. Both emphasize the interconnected nature of various factors, including driver compliance, control parameters, and the MPR of CVs, in determining the efficacy of VSL strategies. In future studies, researchers can explore various aspects to advance the findings of this study and enhance our understanding of preventing or reducing the capacity drop phenomenon at bottlenecks through CV-based VSL control.
In real-world scenarios, the road is often characterized by multiple lanes, and vehicles frequently

change lanes to optimize their driving conditions. Investigating how multi-lane traffic and lane-changing behaviour affect the capacity drop phenomenon can help identify additional factors that contribute to congestion and develop more effective control strategies. Furthermore, exploring the impact of MPR of CVs on VSL control performance in different bottleneck scenarios, such as lane drop bottlenecks, would be valuable. This research focused on a specific type of bottleneck (sag and tunnel bottlenecks), and extending the analysis to other bottleneck configurations can help assess the generalizability of the findings. Another important consideration is accounting for traffic heterogeneity. Recognizing that different vehicle types, driver characteristics, and preferences exhibit varying following behaviours can enhance the implications of the effectiveness of VSL control.

To improve practicality, future studies can focus on developing a closed-loop VSL control system. This system could include intelligent algorithms that dynamically adjust control parameters based on real-time traffic data and feedback to improve control performance. By continuously adapting the control parameters, the VSL system can maintain its efficiency and effectiveness for varying the MPR of CVs. Furthermore, while this study only utilizes the communication between vehicles and infrastructure, considering the information exchange between vehicles themselves (V2V communication) could lead to the development of more efficient and effective control strategies for future transportation systems, enhancing the overall control performance. Future studies can also explore the integration of connected and autonomous vehicles (CAVs) into the VSL control framework. This can involve investigating the benefits of CAVs in terms of their enhanced sensing capabilities, communication capabilities, and ability to coordinate with VSL systems to improve traffic flow and congestion management.

Lastly, examining the long-term effects and sustainability of VSL control is an important area of research. Instead of relying on the queue discharge rate and travel time as performance measures, future studies can explore the link between traffic flow and other critical aspects such as safety, environmental factors, and overall sustainability. Understanding the broader implications of VSL control beyond just flow improvement can provide a more comprehensive assessment of control performance.

Bibliography

Alasiri, F., Zhang, Y., and Ioannou, P. A. (2021). Robust variable speed limit control with respect to uncertainties. *European Journal of Control*, 59:216–226.

Allen, R. W., Harwood, D., Chrstos, J. P., and Glauz, W. D. (2000). The capability and enhancement of vdanl and twopas for analyzing vehicle performance on upgrades and downgrades within ihsdm. Technical report, Turner-Fairbank Highway Research Center.

Brilon, W. and Bressler, A. (2004). Traffic flow on freeway upgrades. *Transportation research record*, 1883(1):112–121.

Carlson, R. C., Papamichail, I., Papageorgiou, M., and Messmer, A. (2010). Optimal mainstream traffic flow control of large-scale motorway networks. *Transportation Research Part C: Emerging Technologies*, 18(2):193–212.

Chen, D. and Ahn, S. (2018). Capacity-drop at extended bottlenecks: Merge, diverge, and weave. *Transportation Research Part B: Methodological*, 108:1–20.

Chen, D., Ahn, S., and Hegyi, A. (2014). Variable speed limit control for steady and oscillatory queues at fixed freeway bottlenecks. *Transportation Research Part B: Methodological*, 70:340–358.

Gipps, P. G. (1981). A behavioural car-following model for computer simulation. *Transportation Research Part B: Methodological*, 15(2):105–111.

Goñi-Ros, B., Knoop, V. L., Shiomi, Y., Takahashi, T., van Arem, B., and Hoogendoorn, S. P. (2016). Modeling traffic at sags. *International Journal of Intelligent Transportation Systems Research*, 14:64–74.

Goñi-Ros, B., Knoop, V. L., van Arem, B., and Hoogendoorn, S. P. (2013). Car-following behavior at sags and its impacts on traffic flow. In *presented at the 92nd Annual Meeting of the Transportation Research Board*.

Goñi Ros, B., Knoop, V. L., van Arem, B., and Hoogendoorn, S. P. (2014). Empirical analysis of the causes of stop-and-go waves at sags. *IET Intelligent Transport Systems*, 8(5):499–506.

Goñi-Ros, B., Knoop, V. L., van Arem, B., and Hoogendoorn, S. P. (2014). Mainstream traffic flow control at sags. *Transportation Research Record*, 2470(1):57–64.

Grumert, E. and Tapani, A. (2012). Impacts of a cooperative variable speed limit system. *Procedia-Social and Behavioral Sciences*, 43:595–606.

Grumert, E. F. and Tapani, A. (2017). Using connected vehicles in a variable speed limit system. *Transportation research procedia*, 27:85–92.

Grumert, E. F. and Tapani, A. (2020). Bottleneck mitigation through a variable speed limit system using connected vehicles. *Transportmetrica A: transport science*, 16(2):213–233.

Habtemichael, F. G. and de Picado Santos, L. (2013). Safety and operational benefits of variable speed limits under different traffic conditions and driver compliance levels. *Transportation research record*, 2386(1):7–15.

Hall, F. L. and Agyemang-Duah, K. (1991). Freeway capacity drop and the definition of capacity. *Transportation research record*, (1320).

Han, Y., Chen, D., and Ahn, S. (2017). Variable speed limit control at fixed freeway bottlenecks using connected vehicles. *Transportation Research Part B: Methodological*, 98:113–134.

Haut, B., Bastin, G., and Chitour, Y. (2005). A macroscopic traffic model for road networks with a representation of the capacity drop phenomenon at the junctions. *IFAC Proceedings Volumes*, 38(1):114–119.

Hegyi, A., De Schutter, B., and Hellendoorn, J. (2005). Optimal coordination of variable speed limits to suppress shock waves. *IEEE Transactions on intelligent transportation systems*, 6(1):102–112.

Hegyi, A. and Hoogendoorn, S. P. (2010). Dynamic speed limit control to resolve shock waves on freeways-field test results of the specialist algorithm. In *13th International IEEE Conference on Intelligent Transportation Systems*, pages 519–524. IEEE.

Hegyi, A., Hoogendoorn, S. P., Schreuder, M., Stoelhorst, H., and Viti, F. (2008). Specialist: A dynamic speed limit control algorithm based on shock wave theory. In *2008 11th international ieee conference on intelligent transportation systems*, pages 827–832. IEEE.

Hellinga, B. and Mandelzys, M. (2011). Impact of driver compliance on the safety and operational impacts of freeway variable speed limit systems. *Journal of transportation engineering*, 137(4):260–268.

Helly, W. (1959). Simulation of bottlenecks in single-lane traffic flow.

Jin, W.-L. (2016). On the equivalence between continuum and car-following models of traffic flow. *Transportation Research Part B: Methodological*, 93:543–559.

Jin, W.-L. (2017). A first-order behavioral model of capacity drop. *Transportation Research Part B: Methodological*, 105:438–457.

Jin, W.-L. (2018). Kinematic wave models of sag and tunnel bottlenecks. *Transportation research part B: methodological*, 107:41–56.

Jin, W.-L. and Laval, J. (2018). Bounded acceleration traffic flow models: A unified approach. *Transportation Research Part B: Methodological*, 111:1–18.

Khondaker, B. and Kattan, L. (2015). Variable speed limit: an overview. *Transportation Letters*, 7(5):264–278.

Koshi, M. (1985). Traffic flow phenomena in expressway tunnels. *IATSS research*, 9(1):50–56.

Koshi, M. (2003). An interpretation of a traffic engineer on vehicular traffic flow. In *Traffic and Granular Flow'01*, pages 199–210. Springer.

Koshi, M., Kuwahara, M., and Akahane, H. (1992). Capacity of sags and tunnels on japanese motorways. *ite Journal*, 62(5):17–22.

Lee, J. and Park, B. B. (2013). Evaluation of variable speed limit under connected vehicle environment. In *2013 International Conference on Connected Vehicles and Expo (ICCVE)*, pages 966–967. IEEE.

Letter, C. and Elefteriadou, L. (2017). Efficient control of fully automated connected vehicles at freeway merge segments. *Transportation Research Part C: Emerging Technologies*, 80:190–205.

Li, Y., Shi, Y., Lee, J., Yuan, C., and Wang, B. (2022). Safety effects of connected and automated vehicle-based variable speed limit control near freeway bottlenecks considering driver's heterogeneity. *Journal of advanced transportation*, 2022.

Lighthill, M. J. and Whitham, G. B. (1955). On kinematic waves ii. a theory of traffic flow on long crowded roads. *Proceedings of the Royal Society of London. Series A. Mathematical and Physical Sciences*, 229(1178):317–345.

Lu, N., Cheng, N., Zhang, N., Shen, X., and Mark, J. W. (2014). Connected vehicles: Solutions and challenges. *IEEE internet of things journal*, 1(4):289–299.

Lu, X.-Y., Varaiya, P., Horowitz, R., Su, D., and Shladover, S. E. (2011). Novel freeway traffic control with variable speed limit and coordinated ramp metering. *Transportation Research Record*, 2229(1):55–65.

Marczak, F., Leclercq*, L., and Buisson, C. (2015). A macroscopic model for freeway weaving sections. *Computer-Aided Civil and Infrastructure Engineering*, 30(6):464–477.

Martínez, I. and Jin, W.-L. (2018). Impact of vsl location on capacity drop: A case of sag and tunnel bottlenecks. *Transportation research procedia*, 34:12–19.

Martínez, I. and Jin, W.-L. (2020). Optimal location problem for variable speed limit application areas. *Transportation Research Part B: Methodological*, 138:221–246.

Oh, S. and Yeo, H. (2012). Estimation of capacity drop in highway merging sections. *Transportation research record*, 2286(1):111–121.

Ozaki, H. (2003). Modeling of vehicular behavior from road traffic engineering perspectives. In *Traffic and Granular Flow'01*, pages 281–292. Springer.

Papageorgiou, M., Hadj-Salem, H., Blosseville, J.-M., et al. (1991). Alinea: A local feedback control law for on-ramp metering. *Transportation research record*, 1320(1):58–67.

Papageorgiou, M., Kosmatopoulos, E., and Papamichail, I. (2008). Effects of variable speed limits on motorway traffic flow. *Transportation Research Record*, 2047(1):37–48.

Park, H. and Smith, B. L. (2012). Investigating benefits of intellidrive in freeway operations: Lane changing advisory case study. *Journal of Transportation Engineering*, 138(9):1113–1122.

Rämä, P. (1999). Effects of weather-controlled variable speed limits and warning signs on driver behavior. *Transportation Research Record*, 1689(1):53–59.

Robinson, R. (1984). Problems in the urban environment: traffic congestion and its effects.

Sadat, M. and Celikoglu, H. B. (2017). Simulation-based variable speed limit systems modelling: an overview and a case study on istanbul freeways. *Transportation research procedia*, 22:607–614.

Smulders, S. (1992). Control by variable speed signs: the dutch experiment. In *International Conference on Road Traffic Monitoring and Control (6th: 1992: London, England). 6th International Conference on Road Traffic Monitoring and Control*.

Sun, J., Li, T., Yu, M., and Zhang, H. M. (2018). Exploring the congestion pattern at long-queued tunnel sag and increasing the efficiency by control. *IEEE Transactions on Intelligent Transportation Systems*, 19(12):3765–3774.

Treiber, M., Hennecke, A., and Helbing, D. (2000). Congested traffic states in empirical observations and microscopic simulations. *Physical review E*, 62(2):1805.

Van den Hoogen, E. and Smulders, S. (1994). Control by variable speed signs: results of the dutch experiment.

Wada, K., Martínez, I., and Jin, W.-L. (2020). Continuum car-following model of capacity drop at sag and tunnel bottlenecks. *Transportation research part C: emerging technologies*, 113:260–276.

Wang, M. (2014). Generic model predictive control framework for advanced driver assistance systems.

Wang, M., Daamen, W., Hoogendoorn, S. P., and van Arem, B. (2016). Connected variable speed limits control and car-following control with vehicle-infrastructure communication to resolve stop-and-go waves. *Journal of Intelligent Transportation Systems*, 20(6):559–572.

Xing, J., Muramatsu, E., and Harayama, T. (2014). Balance lane use with vms to mitigate motorway traffic congestion. *International journal of intelligent transportation systems research*, 12(1):26–35.

Xing, J., Takahashi, H., and Takeuchi, T. (2007). Increasing bottleneck capacity through provision of bottleneck location information. In *11th World Conference on Transport ResearchWorld Conference on Transport Research Society*.

Yoshizawa, R., Shiomi, Y., Uno, N., Iida, K., and Yamaguchi, M. (2012). Analysis of car-following behavior on sag and curve sections at intercity expressways with driving simulator. *International Journal of Intelligent Transportation Systems Research*, 10:56–65.

Yuan, K., Knoop, V. L., Leclercq, L., and Hoogendoorn, S. P. (2017). Capacity drop: a comparison between stop-and-go wave and standing queue at lane-drop bottleneck. *Transportmetrica B: transport dynamics*, 5(2):145–158.

Zackor, H. (1991). Speed limitation on freeways: Traffic-responsive strategies. In *Concise Encyclopedia of Traffic & Transportation Systems*, pages 507–511. Elsevier.

A

The table of results

Table A.1: Summary of simulation results for scenario 5 ($1500m$ tunnel bottleneck)

MPR	Applied speed limit (km/h)	Optimal acceleration length from simulation (m)	Increased acceleration length compared to one required in 100% MPR
100%	27.5 (VSL_{max})	1140	/
	27.3	750	/
	27.1	440	/
	26.9	190	/
	26.7	0	/
	23.2 (VSL_{min})	0	/
75%	27.5 (VSL_{max})	1500	360
	27.3	840	90
	27.1	475	35
	26.9	190	0
	26.7	0	0
	23.2(V_{min})	0	0
50%	27.5 (V_{max})	2485	1345
	27.3	1120	370
	27.1	685	245
	26.8	290	245
	26.6	0	0
	23.2 (V_{min})	0	0
25%	27.5	/	/
	27.1	1800	1360
	26.8	750.0	705
	26.5	500.0	500
	26.2	350	350
	25.7	0	0
	23.2 (V_{min})	0	0

Table A.2: Overview of scenario 5 with adjusted parameters ($500m$ tunnel bottleneck)

MPR	Applied speed limit (km/h)	Optimal acceleration length(m)
100%	48.5	3060
	46.5	1165
	43.6	380
	40.2	0
	36.5	0
75%	48.5	5000
	46.5	1325
	43.6	430
	40.2	0
	36.5	0
50%	48.5	/
	46.5	1400
	43.6	480
	40.2	0
	36.5	0
25%	48.5	/
	46.5	2250
	43.6	580
	40.2	0
	36.5	0

B

Matlab Code

```
%----------------define variables
% t:time(s); k:density(veh/km); v:speed(km/h);
L = 1500.0;                    %L:bottleneck length(m);
u = 80.0/3.6;                      %u:free flow speed(m/s);
jd = 140.0/1000.0;                     %jd:jam density(veh/m);
d = 1/jd;                     % jam space
ts1 = 1.5;                   %ts1:timegap at the bottleneck entry(s);
ts2 = 2.1;                   %ts2: timegap at the bottleneck end(s
% ts2 = 2.5;
dts = ts2-ts1;
a0 = 0.407;                   % initialization of acceleration
% a0 = 0.32*0.407;
g = 9.8;
dn = 0.2;
dt = 0.01;
% dn = 0.1;                     % equivalent continumm model
% dt = 0.005;                     % timesteps
totaltime = 1100.0;                 % total duration of observation
% c = (u*jd)./(1+u*jd*timespace);    % location-dependent capacity
c1 = 2000/3600.0; % capacity at the bottleneck entry
c2 = 1500/3600.0; % capacity at the bottleneck end
c3 = 1380/3600.0;
demand= 1.15*c2;

% demand = 0.8*c2 + (1.2*c2-0.8*c2)*rand(1,1);  %generate the random demand between[0.8c2,1.2
    c2]
vn = 250;
% vn = demand*totaltime;
t = [0:dt:totaltime];
n = [0:dn:vn];

%-------------MPR------%
MPR =0.2; % determine the MPR of CVs
total_CV = round(MPR*vn);
allveh = randperm(vn);
CVn = sort(allveh(1:total_CV));          % integer CV
for zz =1:total_CV
    CV(((zz-1)/dn+1):(zz/dn)) = [((CVn(zz)-1)/dn+1):CVn(zz)/dn];  %all CVs including virtual
        vehicles
end

% figure(101)
% NCVn = setdiff([1:vn],CVn);
% % plot([1:vn],zeros(vn,1),'r.');hold on;
% plot(NCVn,ones(vn-total_CV,1)*0.9,'r.');hold on;
% plot(CVn,ones(total_CV,1),'b.')
% ylim([0.8,1.2])
% figure(102)
% bar(CVn,ones(total_CV,1))

```

```
%% ---------------- Variable speed limit ----------------%%
% y = ((a0*jd^2*L)/dts)^(1/3);     %a0 determined by A(x,v)
%c3 = (1/ts2)*(1-1/(1+ts2*y));    %theoretically dropped capacity/lower bound
Vmin = c3/(jd*(1-c3*ts1));       %Minimal speed limit
Vmax = u/(u*jd*dts+1);           %Maximal speed limit
%Vmin = 0.831*Vmax;
if demand>0.99*c2                    % on/off of the speed limit
             VSL= 0.985*Vmax;
%            VSL = u;
else
    VSL = u;
end
Cv = jd*VSL/(jd*ts1*VSL+1);  %Controlled flow
%
%
% %-----------optimal location------%
% vopt(1) = VSL;
% vend = VSL/(jd*VSL*(ts1-ts2)+1);
% pos(1) = 0;
% for ii = 2:length(t)
%    aopt(ii-1) = a0*(1-vopt(ii-1)/u);
% %      aopt(ii-1) = a0;
%     vopt(ii) = vopt(ii-1)+aopt(ii-1)*dt;
%     pos(ii) = pos(ii-1)+vopt(ii-1)*dt;
% end
% [vv,ll] = min(abs(vopt-vend));
% if vopt(ll)>vend
%     La = 1.05*(interp1([vopt(ll-1),vopt(ll)],[pos(ll-1),pos(ll)],vend,'linear')-L);
% else
%     La = 1.05*(interp1([vopt(ll),vopt(ll+1)],[pos(ll),pos(ll+1)],vend,'linear')-L);
% end
% % La=0;
La=5800;
La=max(0,La);


%-------------initialization  activiate the VSL
cf(1).data(1,1) = -La-300;  % the location of the leader car at start time
cf(1).data(2,1) = u;
cf(1).data(3,1) = 0;         % actual acceleration of the leader car at start time
  cf(1).data(4,1) = a0*(1-cf(1).data(2,1)/u);% maximal acceleration of the leader car at
      start time
%  cf(1).data(4,1) = a0;% maximal acceleration of the leader car at start time
for jj=2:length(n)                      % the actual location,speed of the following car at
    start time
        cf(jj).data(1,1) = -La-300-(jj-1)*dn*u/demand;
        cf(jj).data(2,1) = u;
        cf(jj).data(3,1) = 0;    % the actual acceleration of the following car at start time
         cf(jj).data(4,1)= a0*(1-cf(jj).data(2,1)/u);
%         cf(jj).data(4,1)= a0;
end
%-------------car-following
for ii=2:length(t)
     if  cf(1).data(1,ii-1) <= -La && cf(1).data(1,ii-1)>= -La-100 %located in the VSL zone
        if ismember(1,CV)==1
            cf(1).data(2,ii) = min((cf(1).data(2,ii-1)+cf(1).data(4,ii-1)*dt), VSL);
        else
            cf(1).data(2,ii) = min((cf(1).data(2,ii-1)+cf(1).data(4,ii-1)*dt), u);
        end
     else
        cf(1).data(2,ii) = min((cf(1).data(2,ii-1)+cf(1).data(4,ii-1)*dt), u);
    end
    cf(1).data(4,ii) =a0*(1-cf(1).data(2,ii)/u);
%     cf(1).data(4,ii) =a0;
    cf(1).data(1,ii) = cf(1).data(1,ii-1)+cf(1).data(2,ii-1)*dt;
    for jj=2:length(n)
        if cf(jj).data(1,ii-1)<=0
            ts = ts1;
%              cf(jj).data(4,ii-1)= a0;
             cf(jj).data(4,ii-1)= a0*(1-cf(jj).data(2,ii-1)/u);
        elseif cf(jj).data(1,ii-1)>=0 && cf(jj).data(1,ii-1)<=L
```

```
118             ts = ts1+ cf(jj).data(1,ii-1)*dts/L;
119 %              cf(jj).data(4,ii-1)= a0;
120               cf(jj).data(4,ii-1)= a0*(1-cf(jj).data(2,ii-1)/u);
121         else
122             ts = ts1;
123 %             cf(jj).data(4,ii-1)= a0;
124            cf(jj).data(4,ii-1)= a0*(1-cf(jj).data(2,ii-1)/u);
125         end
126
127         s = (cf(jj-1).data(1,ii-1)- cf(jj).data(1,ii-1))/dn;
128         v1 = min(u,1/ts*(s-d));
129         v2 =cf(jj).data(2,ii-1)+cf(jj).data(4,ii-1)*dt;
130         if ismember(jj,CV) == 1 % if vehicles are CVs, their speeds are controlled by speed
                limit in VSL zone
131             if cf(jj).data(1,ii-1)>=-La-100 && cf(jj).data(1,ii-1)<=-La
132                 cf(jj).data(2,ii) = min([v1,v2,VSL]);
133             else
134                 cf(jj).data(2,ii) = min(v1,v2);
135             end
136         else   % if vehicles are NCVs, their speeds are always determined by car following
137             cf(jj).data(2,ii) = min(v1,v2);
138         end
139         cf(jj).data(1,ii) = cf(jj).data(1,ii-1)+ cf(jj).data(2,ii)*dt;   % acctual position
140         cf(jj).data(3,ii-1) = (cf(jj).data(2,ii)-cf(jj).data(2,ii-1))/dt; % actual
                acceleration
141         cf(jj).data(5,ii) = v1;
142         cf(jj).data(6,ii) = s;
143
144     end
145 end
146 % %-------------flow rate at end of sag
147 for jj=1:(1/dn):length(n)    % the time for the jjth vehicle passing the end of bottleneck
148     if cf(jj).data(1,length(t)-1)>1500
149         [m,tt] = min(abs(cf(jj).data(1,(1:(length(t)-1)))-1500));
150         if cf(jj).data(1,tt)>1500
151             %pass_time(jj) = t(tt-1)+dt*(1500-cf(jj).data(1,tt-1))/(cf(jj).data(1,tt)-cf(jj).
                    data(1,tt-1));
152             pass_time(jj)= interp1([cf(jj).data(1,tt-1),cf(jj).data(1,tt)],[t(tt-1),t(tt)
                    ],1500,'linear');
153         else
154             %pass_time(jj) = t(tt)+dt*(1500-cf(jj).data(1,tt))/(cf(jj).data(1,tt+1)-cf(jj).
                    data(1,tt));
155             pass_time(jj)= interp1([cf(jj).data(1,tt),cf(jj).data(1,tt+1)],[t(tt),t(tt+1)
                    ],1500,'linear');
156         end
157     end
158 end
159 pass_time(:,all(pass_time==0,1))=[];
160 for ii=1:length(pass_time)-1
161     cd(ii) = 1/(pass_time(ii+1)-pass_time(ii)); %calculate the flow rate at x=1500
162 end
163
164
165 figure(1)               % trajectories
166  for jj=1:1/dn:length(n)
167        plot(t,cf(jj).data(1,:));hold on;
168
169  end
170 %  plot(t,cf(101).data(1,:),'-b','linewidth',3);
171 %  plot(t,cf(135).data(1,:),'-m','linewidth',2);
172 %  for jj=501
173 % %  for jj=870:1/dn:length(n)
174 %      plot(t,cf(jj).data(1,:));hold on;
175 %  end
176 xlabel('Time,[sec]');
177 ylabel('Space,[m]')
178 ylim([-1.5*L,5*L/3])
179
180
181
182 figure(2)                % speed-x
```

```
for jj=1:1/dn:length(n)
    plot(cf(jj).data(1,:),cf(jj).data(2,:)*3.6);hold on;
end
%  for jj=1800
%      plot(cf(jj).data(1,(88668:110737)),cf(jj).data(2,(88668:110737))*3.6,'-r','linewidth
    ',2);hold on;
%  end
xlabel('Position,x[m]');
ylabel('Speed,v[km/h]')
legend('veh#1','veh#16','veh#21','veh#27','veh#30','veh#40');
ylim([20,100])
xlim([-2000,7000])



% figure(3)                % timespacing
% for jj=1000
%     plot(t(1,:),0.5*(cf(jj).data(6,:))./cf(jj).data(2,:));hold on;
% end


% figure(4)                   % the queue discharge flow rate at x=L
%     plot(t,cd);hold on;

%
figure(5)                    % the normalized queue discharge flow rate at x=L
plot(pass_time(1:length(pass_time)-1),cd/c2);hold on;

xlabel('Time,[sec]');
ylabel('Normalized flow rate at x=L')
ylim([0.9,1])

% figure(6)                % speed-x
% %for jj=1:length(n)
% for jj=[35:37].*(1/dn)-1
%     plot(cf(jj).data(1,:),cf(jj).data(2,:)*3.6);hold on;
% end
% xlabel('Position,x[m]');
% ylabel('Speed,v[km/h]')
% % legend('veh#2','veh#5','veh#10','veh#20','veh#80','veh#140','veh#200','veh#290');
% ylim([20,80])
% xlim([-2000,5000])
```